Available online at www.sciencedirect.com

ScienceDirect

Geochimica et Cosmochimica Acta 148 (2015) 360–377

Geochimica et Cosmochimica Acta

www.elsevier.com/locate/gca

Variability of carbonate diagenesis in equatorial Pacific sediments deduced from radiogenic and stable Sr isotopes

Janett Voigt *, Ed C. Hathorne, Martin Frank, Hauke Vollstaedt [1], Anton Eisenhauer

GEOMAR Helmholtz Centre for Ocean Research Kiel, Wischhofstr. 1-3, 24148 Kiel, Germany

Received 4 February 2014; accepted in revised form 2 October 2014; available online 13 October 2014

Abstract

The recrystallisation (dissolution–precipitation) of carbonate sediments has been successfully modelled to explain profiles of pore water Sr concentration and radiogenic Sr isotope composition at different locations of the global ocean. However, there have been few systematic studies trying to better understand the relative importance of factors influencing the variability of carbonate recrystallisation. Here we present results from a multi-component study of recrystallisation in sediments from the Integrated Ocean Drilling Program (IODP) Expedition 320/321 Pacific Equatorial Age Transect (PEAT), where sediments of similar initial composition have been subjected to different diagenetic histories.

The PEAT sites investigated exhibit variable pore water Sr concentrations gradients with the largest gradients in the youngest sites. Radiogenic Sr isotopes suggest recrystallisation was relative rapid, consistent with modelling of other sediment columns, as the $^{87}Sr/^{86}Sr$ ratios are indistinguishable (within 2σ uncertainties) from contemporaneous seawater $^{87}Sr/^{86}Sr$ ratios. Bulk carbonate leachates and associated pore waters of Site U1336 have lower $^{87}Sr/^{86}Sr$ ratios than contemporaneous seawater in sediments older than 20.2 Ma most likely resulting from the upward diffusion of Sr from older recrystallised carbonates. It seems that recrystallisation at Site U1336 may still be on-going at depths below 102.5 rmcd (revised metres composite depth) suggesting a late phase of recrystallisation. Furthermore, the lower Sr/Ca ratios of bulk carbonates of Site U1336 compared to the other PEAT sites suggest more extensive diagenetic alteration as less Sr is incorporated into secondary calcite. Compared to the other PEAT sites, U1336 has an inferred greater thermal gradient and a higher carbonate content. The enhanced thermal gradient seems to have made these sediments more reactive and enhanced recrystallisation.

In this study we investigate stable Sr isotopes from carbonate-rich deep sea sediments for the first time. Pore water $\delta^{88/86}Sr$ increases with depth (from 0.428‰ to values reaching up to 0.700‰) at Site U1336 documenting an isotope fractionation process during recrystallisation. Secondary calcite preferentially incorporates the lighter Sr isotope (^{86}Sr) leaving pore waters isotopically heavy. The $\delta^{88/86}Sr$ values of the carbonates themselves show more uniform values with no detectable change with depth. Carbonates have a much higher Sr content and total Sr inventory than the pore waters meaning pore waters are much more sensitive to fractionation processes than the carbonates. The $\delta^{88/86}Sr$ results indicate that pore water stable Sr isotopes have the potential to indicate the recrystallisation of carbonate sediments.

* Corresponding author. Tel.: +49 431 600 2242; fax: +49 431 600 2925.

E-mail addresses: jvoigt@geomar.de (J. Voigt), ehathorne@geomar.de (E.C. Hathorne), mfrank@geomar.de (M. Frank), hauke.vollstaedt@csh.unibe.ch (H. Vollstaedt), aeisenhauer@geomar.de (A. Eisenhauer).

[1] Present address: Center for Space and Habitability + Institute of Geological Sciences, University of Bern, Baltzerstr. 1+3, 3012 Bern, Switzerland.

http://dx.doi.org/10.1016/j.gca.2014.10.001

0016-7037/

1. INTRODUCTION

The elemental and isotopic compositions of carbonate microfossils in marine sediments are widely used to reconstruct oceanic and climatic conditions (i.e., temperature, salinity, etc.) in the past (e.g., Zachos et al., 2001, 2008). However, carbonate sediments, mainly coccolithophorid and foraminifera microfossils, are normally altered by recrystallisation during which the original biogenic calcite is replaced by secondary (inorganic) calcite. Significant changes in stable isotope ($\delta^{13}C$ and $\delta^{18}O$) and Mg/Ca ratios of recrystallised planktonic foraminifera have been identified which can lead to biased palaeo-temperatures and to misinterpretations of palaeo-climate (Pearson et al., 2001; Sexton et al., 2006). It is thus essential to better understand the variability of recrystallisation and thereby help to constrain the reliability of proxy data from different sedimentary sections.

The recrystallisation of bulk carbonate sediments has been extensively studied and differences in isotope and element/Ca ratios between altered and well-preserved sediments have been found (e.g., Elderfield et al., 1982; Schrag et al., 1995; Hampt Andreasen and Delaney, 2000). During the recrystallisation of relatively Sr-rich biogenic carbonates Sr^{2+} is released to the pore waters causing the Sr concentration to increase with depth (Baker et al., 1982; Elderfield and Gieskes, 1982; Stout, 1985; Gieskes et al., 1986; Richter, 1993, 1996; Richter and DePaolo, 1987, 1988; Richter and Liang, 1993; Fantle and DePaolo, 2006). To a first order, the slope of the Sr concentration increase indicates the rate of dissolution and re-precipitation or recrystallisation (Richter and DePaolo, 1988). Pore water Sr concentrations and $^{87}Sr/^{86}Sr$ ratios have been used as fitting parameters to constrain models of carbonate recrystallisation (e.g., Baker et al., 1982; Richter and DePaolo, 1987, 1988; Richter and Liang, 1993; Fantle and DePaolo, 2006). Such models estimate the recrystallisation rate, which is defined as the Sr flux from the solid to the fluid (Richter and DePaolo, 1987), by accounting for diffusion, advection and reaction between fluid and solid while adjusting constants to match the observed pore water Sr^{2+} profile (Richter, 1996; Richter and Liang, 1993; Fantle and DePaolo, 2006). All these previous studies show that recrystallisation rates decrease exponentially with increasing depth and age (Baker et al., 1982; Richter and Liang, 1993; Fantle and DePaolo, 2006). Recrystallisation rates are also influenced by sedimentation rates, temperature gradients, lithology and the carbonate saturation state of the overlying bottom waters (Richter and Liang, 1993; Hampt Andreasen and Delaney, 2000). However, the relative importance of these factors for the recrystallisation rate is not well constrained.

Here we investigate recrystallisation by measuring $^{87}Sr/^{86}Sr$ and element/Ca ratios of bulk carbonates and associated pore waters of selected sites of the IODP Expedition 320/321 Pacific Equatorial Age Transect (PEAT) in the eastern equatorial Pacific (Fig. 1). The sediment cores are of similar initial composition at a particular age but have been subjected to different diagenetic histories resulting from variable subsidence, sedimentation rates (Fig. 2) and geothermal gradients. Therefore, these sediments are well suited for the study of recrystallisation.

For the first time, we investigate the stable Sr isotope compositions of carbonate-rich deep sea sediments and their associated pore waters to constrain recrystallisation. By measuring paired radiogenic ($^{87}Sr/^{86}Sr$) and stable ($\delta^{88/86}Sr$) Sr isotopes (Krabbenhöft et al., 2009), natural mass-dependent stable isotope fractionation occurring in the environment can be determined (e.g., Krabbenhöft et al., 2010; Böhm et al., 2012). Recently, stable Sr isotope fractionation has been investigated for biogenic carbonates and inorganic calcite and this suggests a $-0.12‰$ to $-0.25‰$ fractionation between the solid and solution can occur (Krabbenhöft et al., 2010; Böhm et al., 2012; Raddatz et al., 2013).

2. MATERIALS AND METHODS

2.1. Site description

The sites investigated are U1334 to U1338 spanning the late Eocene until present. Sediment cores were recovered

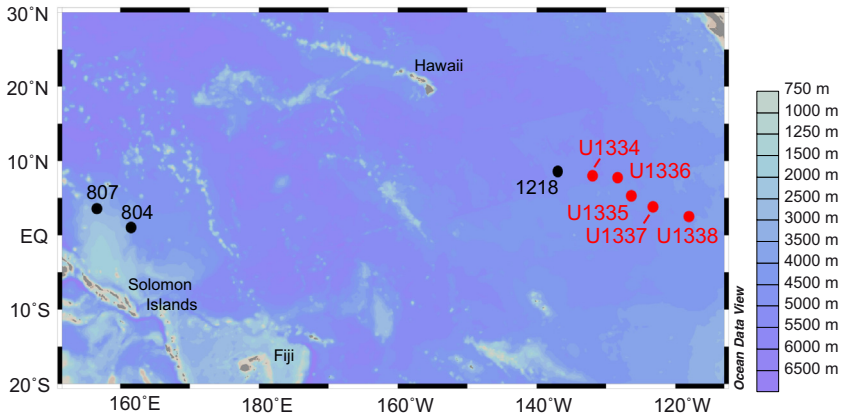

Fig. 1. Map of equatorial Pacific showing the location of PEAT sites (Pälike et al., 2010) investigated in this study in red and ODP Sites 804, 807 (Kroenke et al., 1991) and 1218 (Lyle et al., 2002).

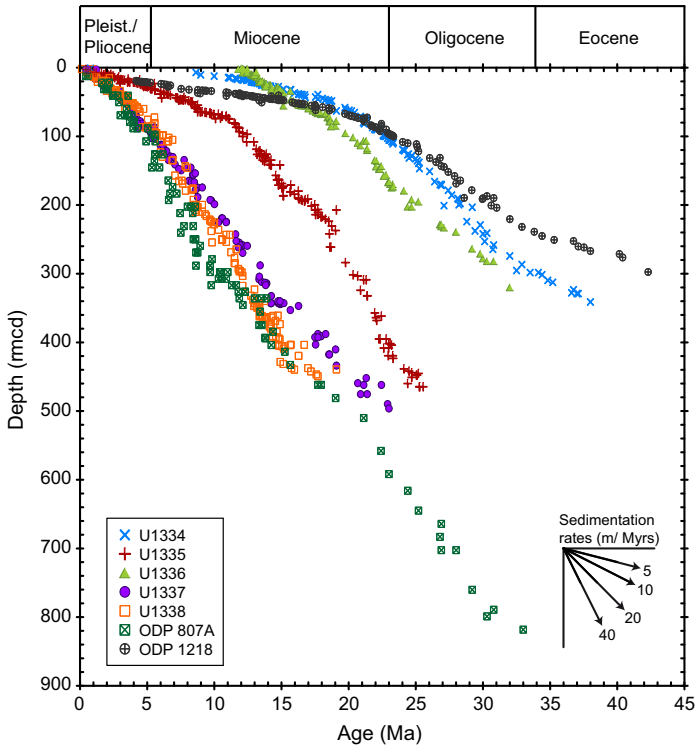

Fig. 2. Sedimentation rates of PEAT sites, age is plotted against revised metres composite depth (rmcd), from Pälike et al. (2010). Revised composite depths are from Westerhold et al. (2012) and Wilkens et al. (2013). ODP Sites 807 (Kroenke et al., 1991) is shown in metres below seafloor (mbsf) and 1218 (Lyle et al., 2002) in metres composite depth (mcd). Both sites were adjusted to the PEAT age scale.

during the IODP Expedition 320/321 and site locations and basic coring data are summarised in Table 1 (Pälike et al., 2010). All depths reported here for the PEAT Sites U1334, U1336, U1337 and U1338 are in revised metres composite depth (rmcd) (Westerhold et al., 2012; Wilkens et al., 2013) and for Site U1335 depth is given in metres composite depth (mcd) (Pälike et al., 2010).

The sedimentary sequences represent a continuous Cenozoic record of the equatorial Pacific recovered along an age transect where different sites were located within a 2° band north and south of the equator for different time intervals (Pälike et al., 2010). The sites were located in the equatorial high productivity zone at different time periods as the Pacific plate moved away from East Pacific Rise. All PEAT sites are relatively carbonate-rich ranging from 40.1% to 97.8% $CaCO_3$ within the ooze sections (Fig. S1). Low carbonate content is found in opal-rich layers at Sites U1335, U1337 and U1338, reaching <1% $CaCO_3$ in places at Site U1337. Generally, the sites consist of nanno- and microfossil ooze with only minor amounts of clay in the top of the sediment sequences. This is most pronounced at Sites U1334 and U1336 where a clay layer accumulated since the site subsided below the carbonate compensation depth (CCD) around 12 Ma (Pälike et al., 2010, 2012). All other sites are at present still above the CCD (Pälike et al., 2010, 2012), the depth where the rate of calcite supply equals the dissolution rate resulting in no calcite accumulation.

Porosity decreases in several steps down hole as a function of compaction from 64% to 91% in the upper sections to about 47–54% near the basement (Fig. S2) (Pälike et al., 2010). The ooze–chalk transition at each site is located at

Table 1
Details of the investigated PEAT Sites (for further information see Pälike et al., 2010).

Site	Geographic location	Water depth (m)	Sediment thickness (m)[a]	Age of underlying crust (Ma)
U1334	7°59.998′N, 131°58.408′W	4799	~285	~38
U1335	5°18.735′N, 126°17.002′W	4328	~420	~26
U1336	7°42.067′N, 128°15.253′W	4286	~174	~32
U1337	3°50.007′N, 123°12.356′W	4461	~450	~24
U1338	2°30.469′N, 117°58.178′W	4200	~413	~18

[a] All Sites, except Site U1336, were drilled to the basement. The sediment thickness represents the total drilling depth below seafloor to the basalt basement.

different depths due to different sedimentation rates and is found at 273.5 rmcd at Site U1334, at 393.4 mcd at Site U1335, at 347.6 rmcd at Site U1337 and at 343.1 rmcd at Site U1338 (Pälike et al., 2010). Site U1336B consists only of ooze since sections deeper than 191.9 rmcd were not drilled (Pälike et al., 2010).

The geothermal gradients vary significantly between the PEAT sites. Sites U1334, U1337 and U1338 have similar geothermal gradients of 33.0, 32.4 and 34.4 °C km^{-1}, respectively (Pälike et al., 2010). Site U1335 has the lowest geothermal gradient of only 7.4 °C km^{-1} (Pälike et al., 2010). Unfortunately, no *in-situ* temperature measurements were conducted at Site U1336 because of time constraints, but pore water Mg^{2+}, Ca^{2+} and K^{+} suggest that this site is relatively reactive and by inference subject to a relatively high thermal gradient (see Section 4.1).

Pore water profiles of Sites U1334, U1335 and U1338 show rather uniform values for Mg^{2+} and Ca^{2+} (Table S1 contains pertinent pore water data, compiled from Pälike et al., 2010). At Site U1336 Ca^{2+} concentrations increase with depth and show a sharp increase at 147.6 rmcd whereas the Mg^{2+} concentrations decrease with depth and show an enhanced gradient of the decrease at the same depth. At Site U1337 many pore water profiles, but not Mg^{2+} and Ca^{2+} values, are offset either side of a chert layer at 263 rmcd (Table S1, see also Section 4.1, Pälike et al., 2010).

Data from Ocean Drilling Program (ODP) Sites 1218, 804 and 807 are compared to the PEAT sites. Detailed information for Site 1218 can be found in Lyle et al. (2002) and for Sites 804 and 807 in Kroenke et al. (1991). ODP Site 1218 is also located in the eastern equatorial Pacific about 380 km northwest of Site U1334. The top of the sediment core comprises 52 m of radiolarian clay with a nannofossil ooze and chalk section below (Lyle et al., 2002). This clay layer, similar to Site U1334, reflects the subsidence of this site below the CCD at around 12 Ma (Lyle et al., 2002; Pälike et al., 2012). The porosity of Site 1218 declines down hole from 88% to 48%. The pore water Ca^{2+} concentrations increase from seawater-like 11 to 14 mM at the basement while Mg^{2+} concentrations decrease from 54 to 49 mM (Table S1, Lyle et al., 2002).

ODP Sites 804 and 807 are located in the western equatorial Pacific on the Ontong Java Plateau. The sediments of these sites are carbonate-rich nannofossil oozes and chalk with up to 93% $CaCO_3$ (Delaney and Linn, 1993; Kroenke et al., 1991). Porosity decreases from 70% to 72% in the uppermost sections of the sediments to about 57% at the basement of Site 804 and to 52% at the basement of Site 807 (Kroenke et al., 1991). The pore water Ca^{2+} increases with depth until the basement from 11 to 21–22 mM at both sites and Mg^{2+} decreases with depth from 53 to 42 mM at Site 804 and to 38 mM at Site 807 (Table S1, Kroenke et al., 1991).

2.2. Pore water extraction and sediment leaching

Pore waters were extracted directly after core recovery on board the *JOIDES Resolution* by either the standard IODP technique whole-round squeezing or inserting Rhizon samplers into the sediment core (see Pälike et al., 2010 for more details). Rhizon samples were not taken for all sites investigated but only for Sites U1334, U1337 and U1338. At Site U1334 Rhizon and the squeezed whole-round samples were taken from different holes which explains slight differences between the data. At Site U1337 both methods give identical results within the uncertainties (see Section 2.3 for reproducibility of International Association for the Physical Sciences of the Ocean (IAPSO) seawater measurements on board) (Pälike et al., 2010). Only pH measurements differ at Site U1337 probably because of the time Rhizon samples waited to be measured (Pälike et al., 2010). In general, squeezed whole round samples agree with Rhizon samples indicating both methods are suitable for the data of interest in this study.

Bulk sediment samples (squeeze cake samples; the remaining sediment following pore water extraction) were processed and analysed at GEOMAR. The samples were freeze dried and about 100 mg were ground for homogenisation. The powder was transferred into acid cleaned 50 ml centrifuge tubes and subjected to a modified leaching method after Kryc et al. (2003).

Sample powders were rinsed three times with 20 ml of deionized 18.2 MΩ water to remove the loosely-bound fraction and were then shaken for 30 min on a shaker table (140 rpm) before being centrifuged for 30 min (4000 rpm). Although the 18.2 MΩ water was slightly acidic (>pH 5.5), it was not observed to be aggressive. The supernatant was discarded. The carbonate fraction was dissolved with 20 ml of 0.1 M acetic acid buffered to pH 5 with sodium acetate. Samples were continuously agitated on a shaker table (125 rpm) for 18 h at room temperature before being centrifuged for about 30 min (4000 rpm) and the supernatant was transferred into acid cleaned Savillex® vials.

2.3. Elemental analysis

Pore water samples were measured for elemental composition on board the *JOIDES Resolution* by inductively coupled plasma atomic emission spectroscopy (ICP-AES) following established techniques (Gieskes et al., 1991; Murray et al., 2000; Pälike et al., 2010). To assess the precision of the ICP-AES technique IAPSO seawater was measured multiple times. The relative standard deviation (RSD, 2σ) for the conservative elements in the IAPSO seawater during the shipboard analyses was ±5.5% for Mg^{2+}, 3.0% for Ca^{2+}, 3.1% for Sr^{2+} and 1.6% for K^{+} (Pälike et al., 2010). To determine the precision for Mn^{2+} and Fe^{2+} some pore waters were repeatedly measured and gave a reproducibility of 16% RSD for Mn^{2+} and 6.6% RSD for Fe^{2+} (Pälike et al., 2010). Alkalinity and pH of the pore waters were determined by Gran titration with a Brinkman pH electrode and Metrohm autotitrator (Pälike et al., 2010).

An aliquot of each bulk carbonate leachate was taken for determination of element/Ca ratios by inductively coupled plasma mass spectrometry (ICP-MS, Agilent 7500cx at GEOMAR) calibrated using multi-element standards made from high purity single element solutions. Uncertainties (2σ) estimated by repeated measurement of a sample are ±2.13% RSD for Mg/Ca ratios, 1.82% for Sr/Ca ratios,

9.35% for Mn/Ca ratios and 10.36% for Fe/Ca ratios (see also Table S2 and figure captions).

2.4. Radiogenic and stable Sr isotope analysis

For multi collector inductively coupled plasma mass spectrometry (MC-ICP-MS) analysis of $^{87}Sr/^{86}Sr$ ratios, an aliquot of the carbonate leachates containing about 500 ng Sr or 100 µl of pore water were dried down, re-dissolved in 100 µl of 8 M HNO_3 and loaded onto chromatographic columns filled with 55 µl of Eichrom SrSpec resin (mesh size: 50–100 µm). The sample matrix was eluted with 8 M HNO_3 and Sr was collected in 1 ml 18.2 MΩ water.

$^{87}Sr/^{86}Sr$ ratios were measured on a *Nu Plasma* MC-ICP-MS. Data were acquired at a typical ^{88}Sr signal intensity of about 8 V and were corrected for mass bias with the $^{86}Sr/^{88}Sr$ ratio of 0.1194 (Nier, 1938) and the exponential law. As is standard practice with MC-ICP-MS, $^{87}Sr/^{86}Sr$ ratios of each analytical session were corrected to the accepted value of the standard SRM 987 = 0.710248 (McArthur and Howarth, 2004) to account for additional fractionation effects and instrument drift between sessions. The SRM 987 is distributed by the National Institute of Standards and Technology (NIST). Repeated measurements of the IAPSO seawater, subjected to the same chemistry as the samples, gave an average $^{87}Sr/^{86}Sr$ value of 0.709171 ± 0.000019 (2σ, $n = 51$).

Paired Sr isotope analyses ($^{87}Sr/^{86}Sr$, $\delta^{88/86}Sr$) followed the procedure from Krabbenhöft et al. (2009). Sample solutions containing about 1200 ng Sr were dried down and re-dissolved in 2 ml of 8 M HNO_3 and split into two aliquots. One aliquot was spiked with a $^{87}Sr/^{84}Sr$ double spike. Sr separation from the sample matrix was performed as described above but using about 200 µl of the Eichrom SrSpec resin and the Sr was collected in 4 ml of 18.2 MΩ water. After separation solutions were dried down and 200 µl of 8 M HNO_3 and 100 µl of H_2O_2 (30%) were added and heated at 80 °C for at least 6 h to break down any residual resin or other organic material. Finally, the samples were dried down again and about 300 ng Sr loaded onto single Re filaments with H_3PO_4 and $TaCl_5$ activators.

Measurements were performed by thermal ionisation mass spectrometry (TIMS, Triton) at about 1400 °C with a typical ^{88}Sr signal intensity of about 10 V. Spike correction and normalisation to the NIST SRM 987 ($^{88}Sr/^{86}Sr$ of 8.375209 (Nier, 1938)) were carried out after Krabbenhöft et al. (2009) to calculate the $\delta^{88/86}Sr$ of the samples and reference materials. Simultaneously measured $^{87}Sr/^{86}Sr$ ratios were also corrected for mass bias using $^{86}Sr/^{88}Sr = 0.1194$ (Nier, 1938). Repeated measurement of the NIST SRM 987 standard gave an average $^{87}Sr/^{86}Sr = 0.710246 \pm 0.000022$ (2σ, $n = 16$). The $^{88}Sr/^{86}Sr$ ratios are reported in the common delta notation relative to the SRM 987: $\delta^{88/86}Sr\ (‰) = [(^{88}Sr/^{86}Sr)_{sample}/(^{88}Sr/^{86}Sr)_{SRM\ 987} - 1] * 1000$. The IAPSO seawater was measured repeatedly and gave an average $\delta^{88/86}Sr$ of 0.381 ± 0.029‰ and $^{87}Sr/^{86}Sr$ of 0.709167 ± 0.000004 (2σ, $n = 5$, see also Table 2) consistent with published values (e.g., Fietzke and Eisenhauer, 2006; Krabbenhöft et al., 2009, 2010). Repeated measurement of the JCp-1 coral reference material gave an average $\delta^{88/86}Sr$ of 0.202 ± 0.027‰, and $^{87}Sr/^{86}Sr = 0.709168 \pm 0.000019$ (2σ, $n = 10$, Table 2) in good agreement with published data (Krabbenhöft et al., 2010). The analytical blank for the leaching procedure and chromatographic Sr separation including the 18.2 MΩ water, acidified on the ship identical to the pore water samples, were determined and contained 0.35 and 0.16 ng Sr, respectively, which is less than 0.1% of the Sr amount in samples.

Table 2
$\delta^{88/86}Sr$ and $^{87}Sr/^{86}Sr$ values of bulk carbonate leachates and associated pore waters as well as standards measured by TIMS.

Sample	Depth (rmcd)	Age (Ma)	Pore waters			Bulk carbonate leachates		
			$^{87}Sr/^{86}Sr$	$\delta^{88/86}Sr$ (‰)	Sr[a] (ppm)	$^{87}Sr/^{86}Sr$	$\delta^{88/86}Sr$ (‰)	Sr[b] (ppm)
U1334A 30X3	330.64	37.04	0.709030	0.473	7.50	0.707739	0.217	1075
U1336B 2H5	9.78	12.73	0.708941	0.428	8.22	0.708829	0.245	1096
U1336B 6H2	50.36	16.30	0.708551	0.505	13.53	0.708707	0.231	1142
U1336B 12H3	113.79	20.90	0.708319	0.635	19.32	0.708321	0.235	1161
U1336B 13H3	125.04	21.56	0.708298	0.655	20.25	0.708298	0.241	1146
U1336B 20H3	186.67	24.36	0.708086	0.700	36.61	0.708137	0.211	1223
U1337A 26X3	258.03	11.91	0.709030	0.605	9.09	0.708840	0.240	1308
U1338A 18H3	179.03	8.22	0.708932	0.457	33.30	0.708935	0.249	1091
U1338B 36H3	359.44	13.84	0.708925	0.365	16.06	0.708822	0.230	1539
IAPSO seawater	–	–	0.709167 ± 0.000004	0.381 ± 0.029	7.45	–	–	–
JCp-1 coral	–	–	–	–	–	0.709168 ± 0.000019	0.202 ± 0.027	

The analytical uncertainties for the pore waters are comparable to those measured for IAPSO seawater reference material and the reproducibility of the bulk carbonates conforms to that of the JCp-1 coral reference material.

[a] The Sr content (ppm) of the pore waters was calculated from the Sr concentration reported from Pälike et al. (2010).

[b] The Sr content (ppm) of the bulk carbonates was calculated from the Sr/Ca ratio and the Ca content from this sample. The Ca content was estimated from the $CaCO_3$ content given by Pälike et al. (2010).

The analytical uncertainties for the pore water measurements were estimated using the IAPSO seawater and the reproducibility of the bulk carbonate analyses was estimated with the JCp-1.

3. RESULTS

3.1. Pore water Sr concentration

The pore water Sr concentrations increase with depth from the sediment water interface to different extents at each site (Fig. 3). The smallest increase is observed at Site U1334 and the greatest occurs at U1338. At most of the PEAT sites the Sr concentration then decreases towards seawater-like values (85 µM) near the basement. This decrease is consistent with relatively fresh seawater circulating through the basement (Pälike et al., 2010). Site U1334 exhibits a small increase with depth reaching maximum values of only 107 µM (Fig. 3) which is still very close to seawater concentrations. The sampled section of U1336 does not show a Sr maximum but rather a continuous increase of the Sr concentration with depth, however with a significantly steeper slope below 137.3 rmcd (Fig. 3). The lower section below 186.7 rmcd at Site U1336 was not sampled for pore waters because of time constraints during the expedition. Site U1338 shows the strongest increase of pore water Sr concentration with depth, as well as the highest Sr^{2+} values observed at PEAT sites of 400 µM (Fig. 3). The peak Sr concentration of this site also occurs at the shallowest depth at about 221.1 rmcd below sea floor (Pälike et al., 2010).

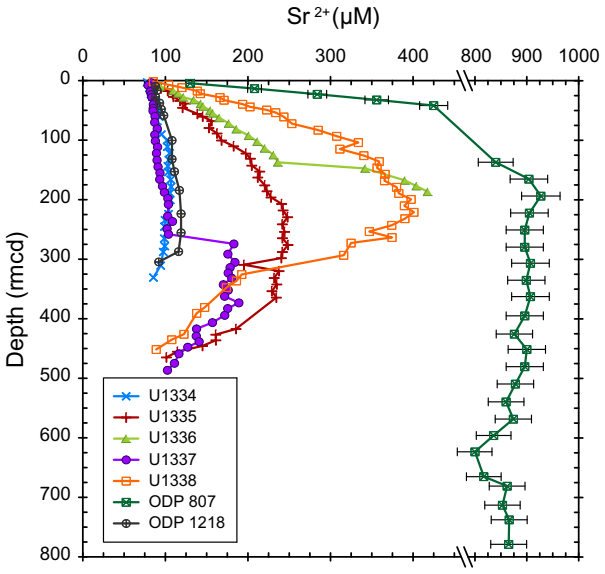

Fig. 3. Pore water Sr concentrations for the PEAT sites investigated (Pälike et al., 2010) and ODP Sites 807 (Kroenke et al., 1991) and 1218 (Lyle et al., 2002) plotted against depth. Revised composite depths are from Westerhold et al. (2012) and Wilkens et al. (2013). Depth scale for ODP Site 807 is mbsf and for Site 1218 is mcd. Error bars of the PEAT sites at 2σ level are ±3.06% (Pälike et al., 2010) and for ODP Site 1218 are ±4.8% (Lyle et al., 2002). The errors for the PEAT sites and Site 1218 are as big as the symbol size. Error bars shown for ODP Site 807 at 2σ level are ±4% (Kroenke et al., 1991).

3.2. $^{87}Sr/^{86}Sr$ ratios of pore waters

Pore water $^{87}Sr/^{86}Sr$ ratios of Sites U1334, U1335 and U1337 have generally more radiogenic (higher) $^{87}Sr/^{86}Sr$ ratios than seawater of contemporaneous age as reflected by marine carbonate sediments globally (McArthur et al., 2001) (Fig. 4a, b, d, Table S3). The ratios decrease from 0.7092 to up to 0.7088 and then increase again towards the basement. Site U1336 pore waters exhibit less radiogenic (lower) $^{87}Sr/^{86}Sr$ ratios than contemporaneous seawater (McArthur et al., 2001) in sediments older than 14.7 Ma (below 32.5 rmcd) with a maximum difference of 0.000143 corresponding to 2.85 Myrs (Fig. 4c). The pore water $^{87}Sr/^{86}Sr$ ratios of Site U1338 are close to contemporaneous seawater in sediments younger than 9.5 Ma and then increase with depth (Fig. 4e).

3.3. $^{87}Sr/^{86}Sr$ ratios ratio of bulk carbonate leachates

The $^{87}Sr/^{86}Sr$ ratios of the bulk carbonates decrease with depth from 0.7092 to 0.7077 and are generally in very good agreement (within 2σ uncertainties) with contemporaneous seawater (McArthur et al., 2001) (Fig. 4, Table S3). However, the carbonate $^{87}Sr/^{86}Sr$ ratios of Site U1336 older than 20.2 Ma exhibit systematically less radiogenic values than contemporaneous seawater (Fig. 4c).

The $^{87}Sr/^{86}Sr$ ratios of the bulk carbonates at Site U1335 are more radiogenic than contemporaneous seawater in places. This may result from turbidites observed in this core (Pälike et al., 2010) transferring younger sediments to greater depths (Fig. 4b). These deviations towards younger seawater $^{87}Sr/^{86}Sr$ ratios occur between 7.1–9.2 Ma (45.5–60.3 mcd), 13.7–14.2 Ma (131–142.6 mcd) and 22.9–23.6 Ma (393–417.1 mcd), although shipboard sedimentology does not suggest any gravity flows in sediments younger than 11.6 Ma (about 89 mcd). This site will not be discussed further regarding recrystallisation because of the disturbed sedimentation.

3.4. Element/Ca ratios of bulk carbonates

The Sr/Ca ratios of the bulk carbonates of the PEAT sites range from 1.23 to 2.96 mmol/mol (Fig. 5a, Table S2). The Sr/Ca ratios of Site U1336 are generally lower than of the other PEAT sites (Fig. 5a). The Sr/Ca ratios of Sites U1334, U1335, U1337 and U1338 fluctuate around 2 mmol/mol interrupted by a transient increase between 8.9 and 11.1 Ma at Sites U1337 and U1338 (Fig. 5a). The highest Sr/Ca value of Site U1338 of nearly 3 mmol/mol coincides with the maximum in the pore water Sr.

The Mg/Ca ratios of the bulk carbonates range from 1.0 to 32.2 mmol/mol (Fig. 5b, Table S2). The Mg/Ca ratios fluctuate around 2–3.5 mmol/mol with a notable deviation between 8.2 and 9.5 Ma at Sites U1337 and U1338 (with the highest value reaching 32 mmol/mol) (Fig. 5b) similar to the excursion in Sr/Ca (Fig. 5a).

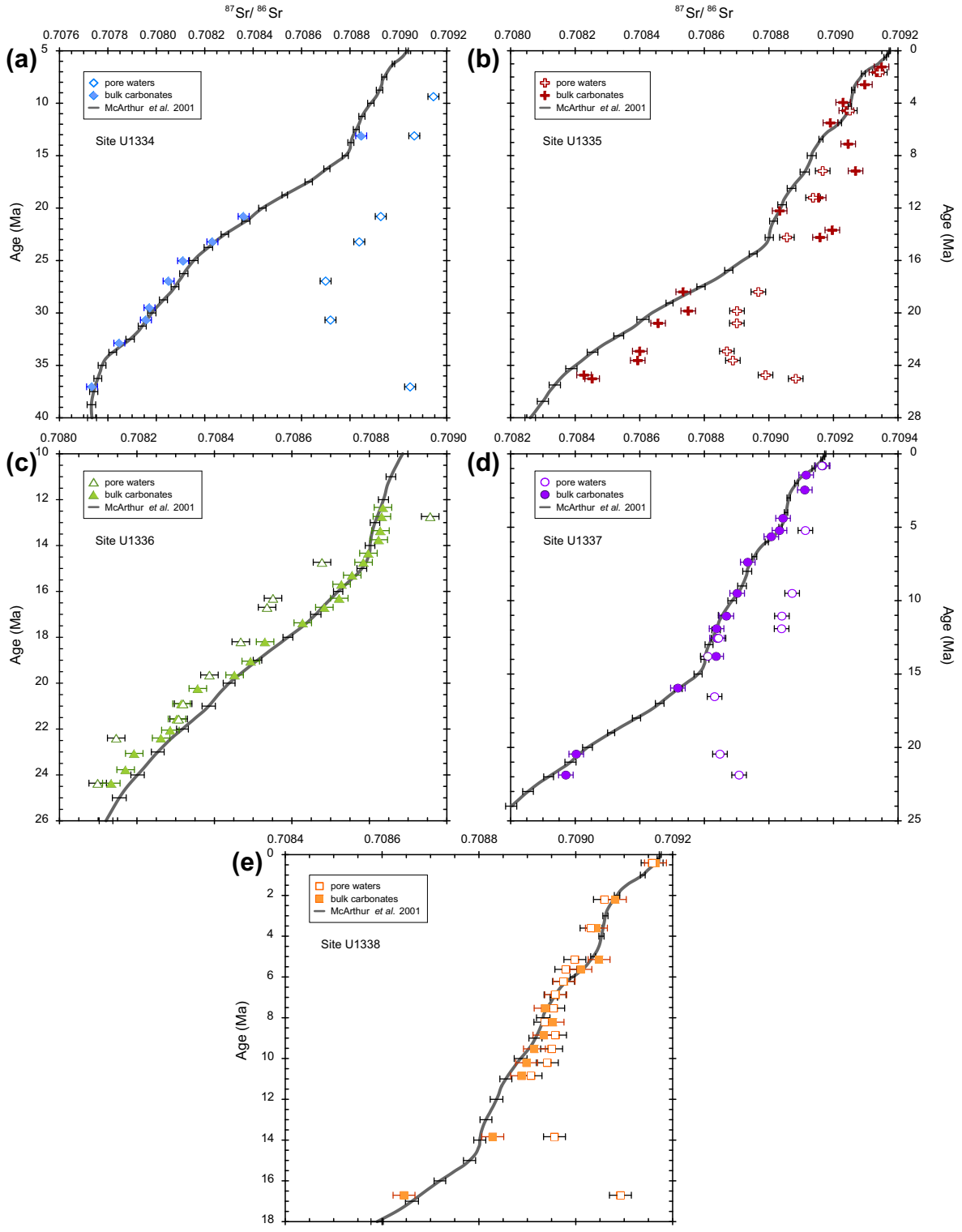

Fig. 4. $^{87}Sr/^{86}Sr$ ratios of the PEAT sites investigated plotted versus age. The seawater Sr isotope curve is shown as a grey line (McArthur et al., 2001, LOWESS fit, version 3) and represents the contemporary seawater composition based on a compilation of 13 published sources for the shown ages. Error bars of the seawater Sr isotope curve represent the 2σ uncertainties of the data compiled by McArthur et al. (2001). Closed symbols represent bulk carbonate leachates and open symbols are pore water samples. Error bars for the PEAT sites denote the 2σ uncertainties of repeated measurements of IAPSO seawater. Please note the different scales for each panel. $^{87}Sr/^{86}Sr$ ratios of the PEAT sites are plotted against depth in Figs. S6 and S7.

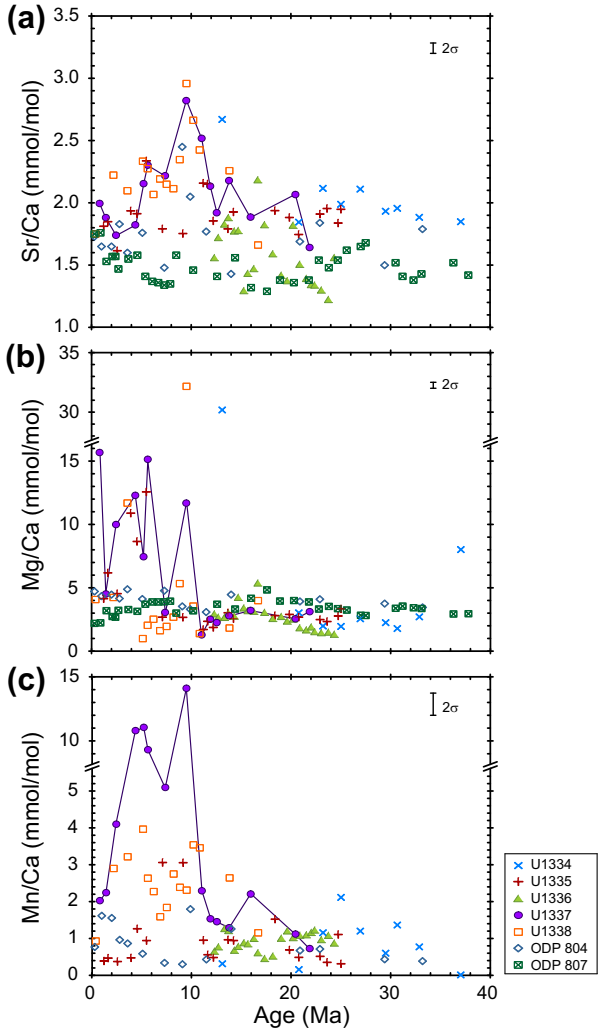

Fig. 5. Sr/Ca (a), Mg/Ca (b) and Mn/Ca (c) ratios of bulk carbonate leachates shown against age. Values from ODP Sites 804 and 807 are from Delaney and Linn (1993). Error bars represent the 2σ uncertainty estimates and were estimated from repeated measurements of one sample. High Sr/Ca and Mg/Ca values between 8 and 11 Ma at Sites U1337 and U1338 are probably related to high productivity events and the dissolution of carbonates (Lyle et al., 1995). This is supported by a low carbonate content (<1 wt %) during this interval at Site U1337 (Pälike et al., 2010) (Fig. S1, Table S2). The peak in Mg/Ca ratios may be caused by diagenetic overgrowths of Mg-rich carbonate (Boyle, 1983; Higgins and Schrag, 2012). Data plotted versus depth (rmcd) are shown in Fig. S8.

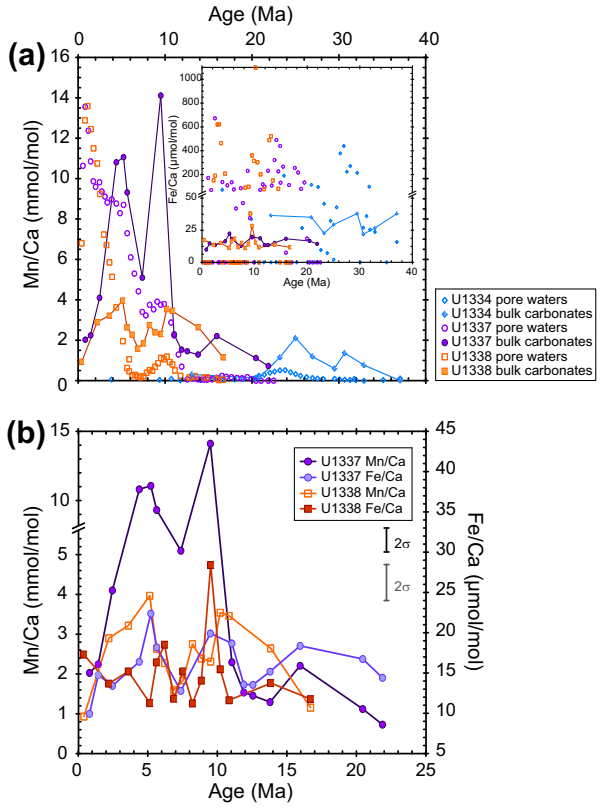

Fig. 6. Mn/Ca (a) and Fe/Ca insert) ratios of bulk carbonate leachates and pore waters of Sites U1334 (blue diamonds), U1337 (purple circles) and U1338 (orange squares) plotted against age. (b) Bulk carbonate Mn/Ca and Fe/Ca of Site U1337 and U1338 plotted against age for direct comparison. Please note the different scale on the *x*-axis in (a) and (b). Closed symbols represent bulk carbonate leachates and open symbols are pore water samples. Data for pore waters are from Pälike et al. (2010). Error bars for Mn/Ca (black) and Fe/Ca (grey) represent the 2σ uncertainty estimates from repeated measurements of one sample. Mn/Ca and Fe/Ca ratios versus depth (rmcd) are illustrated in Fig. S9. (For interpretation of the references to colour in this figure legend, the reader is referred to the web version of this article.)

The Mn/Ca ratios of the bulk carbonates from the PEAT sites range from 0.01 to 14.11 mmol/mol with an excursion between 7.1 and 10.8 Ma at Sites U1335, U1337 and U1338 (Fig. 5c, Table S2). These increases in carbonate Mn/Ca corresponded to intervals of increased dissolved Mn in pore waters (Fig. 6, Table S1).

3.5. $\delta^{88/86}$Sr of pore waters and bulk carbonate leachates

Nine bulk carbonate and associated pore water couplets were chosen for the measurement of $\delta^{88/86}$Sr because both their bulk carbonate and pore water $^{87}Sr/^{86}Sr$ ratios either deviated from the seawater Sr isotope curve or there was a difference in $^{87}Sr/^{86}Sr$ between pore water and bulk carbonate (Fig. 7a, Table 2). One sample (U1338A 18H3, 179 rmcd, 8.2 Ma; Table 2) represents a control sample as both the pore water and the bulk carbonate $^{87}Sr/^{86}Sr$ ratios did not deviate from contemporaneous seawater.

The $\delta^{88/86}$Sr of pore waters analysed from Site U1338 and the shallowest sample of U1336 are relatively close to modern seawater values whereas the analysed pore waters of Sites U1334, U1336 (except the shallowest sample) and U1337 exhibit heavier $\delta^{88/86}$Sr values compared to modern seawater (IAPSO = 0.381 ± 0.029‰, $n = 5$) (Fig. 7, Table 2). Generally, the $\delta^{88/86}$Sr values of U1336 pore waters increase with depth and age (Fig. 7, Table 2).

The $\delta^{88/86}$Sr values of the bulk carbonates do not show a trend with depth or age, ranging from 0.211‰ to 0.249‰

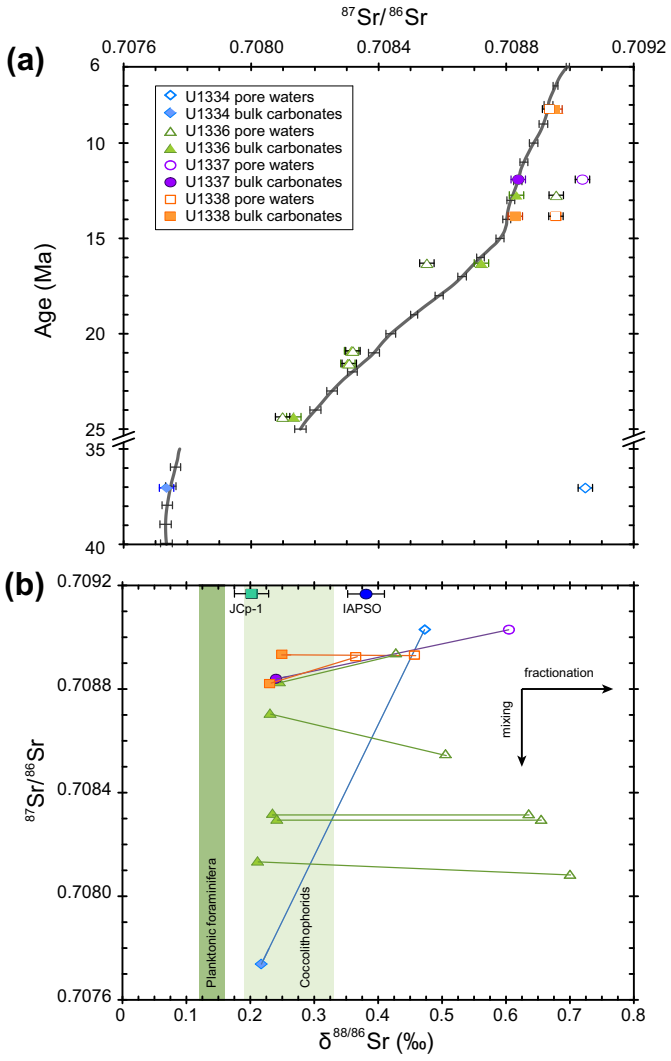

Fig. 7. (a) $^{87}Sr/^{86}Sr$ ratios of the selected bulk carbonate and associated pore water couplets plotted against age. (b) Stable Sr ($\delta^{88/86}Sr$) isotopes of selected bulk carbonate leachates and their associated pore waters from Sites U1334 (blue diamonds), U1336 (green triangles), U1337 (purple circles) and U1338 (orange squares) plotted against the radiogenic Sr ratio ($^{87}Sr/^{86}Sr$). Bulk carbonates and associated pore waters are connected by a line. Closed symbols represent bulk carbonate leachates and open symbols are pore water samples. IAPSO seawater and JCp-1 coral reference material measurements are shown for comparison. The error bars for the IAPSO seawater represent the analytical uncertainties of the pore waters and the uncertainty of the JCp-1 represents those for the bulk carbonates. Coloured bars represent the $\delta^{88/86}Sr$ range of planktonic foraminifera and coccolithophorids (Krabbenhöft et al., 2010; Böhm et al., 2012). The depth and age for each bulk carbonate and associated pore water couplet is given in Table 2. (For interpretation of the references to colour in this figure legend, the reader is referred to the web version of this article.)

and are similar to modern carbonates (coral reference material JCp-1 = 0.202 ± 0.027‰, $n = 10$) (Fig. 7, Table 2).

4. DISCUSSION

4.1. Insights from pore water chemistry

Below the pore water Sr concentration maximum, a decrease with depth is observed for ODP Site 1218 (Lyle et al., 2002) and Sites U1334, U1335, U1337 and U1338 (Fig. 3) where circulation of relatively modern seawater through the basement was inferred from various chemical species in the pore waters like Li^+ and sulphate (Baker et al., 1991; Pälike et al., 2010). This seawater in the basement has a lower Sr^{2+} concentration than the pore waters and the gradient causes diffusive exchange. A trend towards modern seawater values is also seen in the $^{87}Sr/^{86}Sr$ ratios of the pore waters (see Section 4.2). In the case of Site U1336 the lower section of the sediment was not sampled for pore waters.

A small increase in pore water Sr^{2+} may result from net carbonate dissolution in opal-rich layers, especially at Sites U1337 and U1338 (see Fig. 24, Site U1338 in Pälike et al., 2010), but the overall Sr^{2+} trend for these sites reflects recrystallisation, diffusion and advection. The clay content of these sediments is low, but reactions with clay are clearly

visible in the Li^+ profiles (not shown here, see Pälike et al., 2010). These differ from the corresponding Sr^{2+} and Mg^{2+} profiles suggesting clay mineral reactions have little influence on these elements here.

The small increase in Sr^{2+} at ODP Site 1218 (Fig. 3) can possibly be explained by the age of the sediments. Site 1218 travelled out of the equatorial high productivity zone at around 28 Ma (Pälike et al., 2010) and below the CCD around 12 Ma resulting in low sedimentation rates thereafter. Therefore, the sediment layer younger than 28 Ma is thin and diffusion caused excess Sr^{2+} in the pore waters to be lost over time (e.g., Richter and Liang, 1993; Rudnicki et al., 2001; Edgar et al., 2013). Site U1334 is similar to Site 1218 and comprises the oldest sediment sampled of the investigated sites. It is therefore likely that the Sr originally released from the biogenic carbonates has been lost from the sediment over time and the recrystallisation, which decreases exponentially with sediment age (Richter, 1996; Richter and DePaolo, 1988; Richter and Liang, 1993; Fantle and DePaolo, 2006), has not kept up. Additional evidence for this is the radiogenic $^{87}Sr/^{86}Sr$ ratios of the pore waters of Site U1334 where diffusive exchange of Sr from seawater results in pore waters some 12.3 Myrs younger than seawater contemporaneous to the sediments in the upper 120 rmcd (see also Section 4.2). The fact that the pore water $^{87}Sr/^{86}Sr$ ratios are not the same as modern seawater suggests a small contribution of Sr from carbonate recrystallisation.

Although the upper part of the sediment sequence of Site U1337 (until 258 rmcd) is younger than at Site U1334, the observed Sr gradient is comparably low (Fig. 3). Diffusive exchange with seawater seems to have been the dominant process (Richter and Liang, 1993) in this upper layer resulting in low Sr^{2+} concentrations and pore water $^{87}Sr/^{86}Sr$ ratios about 7 Myrs younger than seawater contemporaneous to the sediments, similar to those observed at Site U1334. Below 258 rmcd (11.9 Ma) the pore water Sr^{2+} concentration increases strongly (Fig. 3). This sharp increase marks the onset of a chert layer (at 263 rmcd) which acts as an aquitard or a barrier to diffusion (Pälike et al., 2010). Ca^{2+}, Mg^{2+} and K^+ profiles are not offset below the chert layer like Sr^{2+} (Figs. S3 and S4, Table S1), but the former three species are mostly influenced by diffusive exchange with the basement (Lawrence et al., 1975; Gieskes, 1976; Rudnicki et al., 2001). Sr^{2+}, on the other hand, reflects reactions in the sediments, diffusive exchange and advection while other elements also influenced by reactions with the sediment, such as Li^+, Mn^{2+}, Fe^{2+}, and total alkalinity are offset below the chert layer at Site U1337 (Table S1). The Sr released to the pore waters below that layer can thus only diffuse downwards to the relatively young seawater in the basement.

Site U1338 is located on the youngest basement of the PEAT transect (Pälike et al., 2010) and has the thickest sediment cover deposited from the Miocene to present (Fig. 2). It exhibits the steepest pore water Sr^{2+} gradient (Figs. 3 and 8) and therefore is likely to have the highest recrystallisation rates. Although diagenesis modelling for Site U1337 has not been conducted, the sediment accumulation rates and changes in porosity with depth (until the chert layer

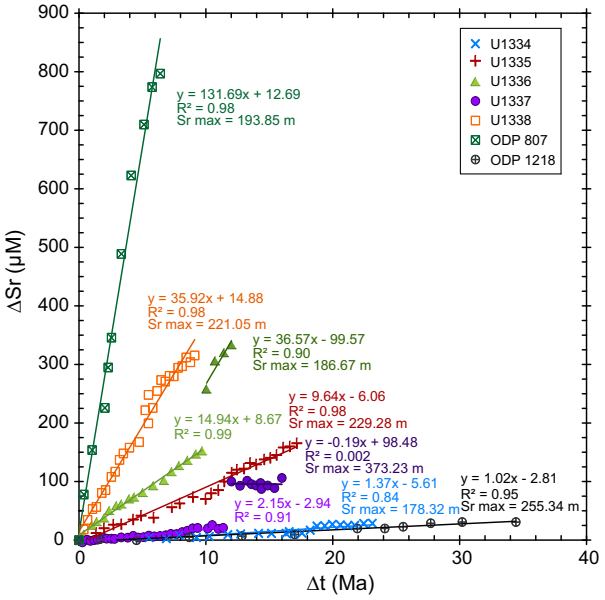

Fig. 8. The change in pore water Sr^{2+} plotted against the change in age of the sediments sampled for waters. The Sr concentration of the shallowest sample was subtracted from the pore water concentration ($\Delta Sr = Sr^{2+}_x - Sr^{2+}_{top}$). Shown ΔSr^{2+} comprises concentrations from the top of the sediment section to the Sr^{2+} maximum depth (given in the plot), except for Site U1336 where all pore water Sr^{2+} values were used. Δt is the age of the core top set to zero for a better comparison between the sites ($\Delta t = t_x - t_{top}$). For Sites U1336 and U1337 two regression lines are shown as the rates change significantly below a layer of restricted diffusional exchange at these sites. The section below this aquitard layer is illustrated by a darker colour. Data for PEAT sites are from Pälike et al. (2010), for ODP Site 1218 from Lyle et al. (2002) and for ODP Site 807 from Kroenke et al. (1991) using the age model from the Initial Reports for the ODP sites (Lyle et al., 2002; Kroenke et al., 1991). (For interpretation of the references to colour in this figure legend, the reader is referred to the web version of this article.)

at 263 rmcd at U1337) (Fig. S2) are very similar for U1338 and U1337, yet the pore water Sr^{2+} gradients differ by a factor of 16. This difference in Sr^{2+} gradients is most likely influenced by the chert layer at Site U1337 preventing Sr^{2+} from below diffusing upwards, but above the chert layer the difference in Sr^{2+} reflects different recrystallisation rates.

The increase in pore water Sr^{2+} concentration with sediment age is shown in Fig. 8. It is likely that Site U1336 would have the deepest Sr^{2+} maximum of all sites, but the total length of the core was not sampled for pore waters. The pore water Sr^{2+} gradient (the slope of the regression lines in Fig. 8) changes with depth at Site U1336 by a factor of 2.6. This change in the pore water Sr^{2+} gradient occurs within a short section of decreased porosity which could restrict the diffusive exchange of the pore water below and above (Gieskes and Lawrence, 1976; Rudnicki et al., 2001). Within this interval, between 137.7 and 142.5 rmcd, the porosity decreases to a mean value of 48.9% compared to 59.6% and 59.9% (mean of 5 m sections) below and above, respectively (Fig. S2) (Pälike et al., 2010). This decrease in porosity is

accompanied by a peak in total organic carbon content of 0.3% at 135.1 rmcd causing a pronounced decline in alkalinity from 2.29 to 1.73 mM by organic material degradation. The decrease in alkalinity and the steeper Sr^{2+} slope suggests higher recrystallisation rates (Richter and DePaolo, 1988). These higher rates may be ascribed to higher temperatures likely at this site since it is located close (about 30 km) to the Clipperton Fracture Zone (Pälike et al., 2010). Although no *in-situ* temperatures were measured at Site U1336, high gradients in pore water Mg/Ca and decreasing K^+ with depth suggest strong reactivity in the basement (Lawrence et al., 1975; Gieskes, 1976; Rudnicki et al., 2001), and comparison to other sites in the region, with negligible horizontal advection in the sediments, suggests a relatively strong thermal gradient for Site U1336 (Fig. 9). This gradient may also have influenced the pore water profiles of Ca^{2+}, Mg^{2+} through reactions with the sediment (Higgins and Schrag, 2012) (Fig. S3, see also Section 4.6). In contrast to Site U1337, the profiles of Ca^{2+} and Mg^{2+} change significantly across the aquitard along with sediment reactive elements like Sr^{2+}, Li^+ and total alkalinity (Fig. S3, Table S1).

Overall, the pore water Sr^{2+} gradient reflects the reactivity to a first order (Fig. 8). ODP Site 807 shows the steepest slope suggesting intense recrystallisation (Delaney and Linn, 1993). The highest pore water Sr^{2+} gradient values of the PEAT transect are observed at Sites U1336 and U1338. To account for variable sediment accumulation rates and vertical advection, sediment diagenesis at both Sites U1336 and U1338 has been simulated using a 1-D reactive transport model (Fig. S5) (J. Higgins personal communication, 2014; Supplementary information and Table S4). The numerical model used to simulate the sediment pore-fluid system is described in detail elsewhere (Higgins and Schrag, 2012). The diagenesis model results suggest Site U1336 is more recrystallised (37% at the bottom of the core at 32 Ma) than Site U1338 (21% at 18 Ma), although only the upper section of Site U1336 could be modelled since the deeper sediment was not sampled for pore waters. The upper sediment column at Site U1336 is more recrystallised which largely results from the sediments having more time to recrystallise than those at Site U1338. The change in the Sr^{2+} gradient below the aquitard, not captured by the model, may be related to the restriction of diffusion, but the continued increase of Sr^{2+} with depth indicates further recrystallisation in the deeper part of the sediment column (see also Section 4.4).

4.2. Radiogenic Sr isotopes of pore waters and bulk carbonate leachates

The bulk carbonate $^{87}Sr/^{86}Sr$ ratios of Sites U1334, U1337, U1338 and the upper sediment column of U1336 (until about 102.5 rmcd, 20.2 Ma) are indistinguishable (within 2σ uncertainties) from contemporaneous seawater (McArthur et al., 2001) indicating that recrystallisation occurred relatively rapidly (within 1.5 Myrs) (Fig. 4). This 1.5 Myrs is based on the analytical uncertainty of the $^{87}Sr/^{86}Sr$ measurements (2σ) converted to age using the McArthur et al. (2001) seawater Sr isotope curve. In

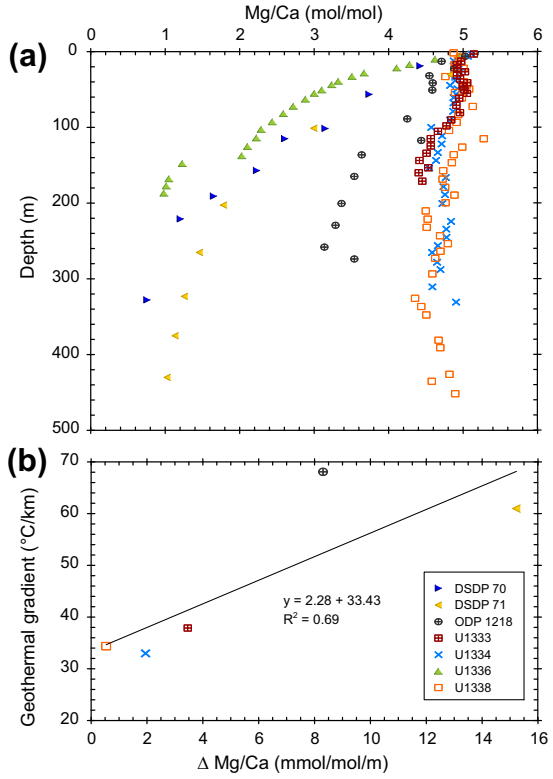

Fig. 9. (a) Pore water Mg/Ca ratios of Deep Sea Drilling Project (DSDP) Sites 70 (blue triangles) and 71 (yellow triangles) (Tracey et al., 1971), ODP Site 1218 (grey crossed circles) (Lyle et al., 2002), and PEAT Sites U1333 (red crossed squares), U1334 (blue crosses), U1336 (green triangles) and U1338 (orange open squares) (Pälike et al., 2010) plotted against depth. The pore water profiles of U1334 and U1338 represent the other PEAT sites investigated as the Mg/Ca profiles are consistent between all sites, except U1336. Depths for PEAT sites are given in rmcd from Westerhold et al. (2012) and Wilkens et al. (2013). Depth scale for DSDP Sites 70 and 71 is mbsf and for ODP Site 1218 is mcd. (b) Pore water Mg/Ca gradient for the first 200 m of the same sites like in a), excluding DSDP Site 70 and U1336, plotted against the geothermal gradient. The pore water Mg/Ca gradient is illustrated for the first 200 m of the sediment column only for better comparison between sites. The gradient was calculated by subtracting the Mg/Ca ratio at surface from the Mg/Ca ratio at 200 m. The geothermal gradient for DSDP Site 71 was taken from Von Herzen et al. (1971). The geothermal gradient for Site 1218 was calculated using the *in-situ* temperature measurements (Lyle et al., 2002) and measured gradients for PEAT sites were taken from Pälike et al. (2010). Also shown is a linear regression for those sites to estimate the geothermal gradient for Site U1336 (78.8 °C km^{-1}). (For interpretation of the references to colour in this figure legend, the reader is referred to the web version of this article.)

sediments younger than 9.5 Ma, the pore waters of Site U1338 show good agreement with contemporaneous seawater (Fig. 4e). All PEAT sites sampled to basement show increasing $^{87}Sr/^{86}Sr$ ratios (towards present-day values) of the pore waters with depth in the oldest parts of the cores confirming the circulation of relatively modern seawater through the basement (Fig. 4a, b, d, e) (Baker et al., 1991). This trend in pore water $^{87}Sr/^{86}Sr$ ratios towards

present-day values shows that the isotopic composition of pore waters can easily be changed by diffusive exchange with young seawater in the basement. It is difficult to change the $^{87}Sr/^{86}Sr$ ratios of bulk carbonates as they have a higher Sr content than pore waters (by a factor of >100, see Table 2). Even in the deeper sediment sections with more radiogenic pore water $^{87}Sr/^{86}Sr$ ratios, the bulk carbonates have not incorporated detectable amounts of pore water Sr.

4.3. Elemental ratios of bulk carbonates

Sr/Ca ratios of bulk carbonates have been used to assess recrystallisation processes, as well as past changes in seawater chemistry (Baker et al., 1982; Delaney, 1989; Delaney and Linn, 1993). The Sr/Ca ratio is species-specific in foraminifera and coccoliths (Stout, 1985; Delaney, 1989; Reinhardt et al., 2000; Stoll and Schrag, 2000) and thus the Sr/Ca will reflect the main constituents when bulk carbonates are measured (Reinhardt et al., 2000). The Sr/Ca ratio is species dependent because of unique calcification processes and calcification rates (Elderfield et al., 1982; Stoll et al., 1999). Recent foraminifera exhibit Sr/Ca values of 1–2 mmol/mol (e.g., Rosenthal et al., 1997; Russell et al., 2004) whereas modern coccolithophorids have Sr/Ca ratios varying from 1.9 to 3.2 mmol/mol (Stoll et al., 2002).

Diagenetic alteration is generally accompanied by lower Sr/Ca ratios in bulk carbonates as less Sr is incorporated into secondary calcite (e.g., Baker et al., 1982; Delaney, 1989). ODP Site 807 is considered to be heavily recrystallised based on Sr/Ca ratios (Delaney and Linn, 1993) and it has been suggested that equilibrium has been achieved between pore waters and carbonate sediments below 150 metres below seafloor (mbsf) (Fantle and DePaolo, 2006). By comparison, the generally lower Sr/Ca ratios of bulk carbonates of Site U1336, which are similar to those of Site 807, suggest more extensive diagenetic alteration compared to the other PEAT sites (Fig. 5a). Site U1336 Sr/Ca decreases slightly with depth indicating further recrystallisation. In contrast, the bulk carbonate samples of Site U1334 exhibit higher Sr/Ca ratios suggesting a better preservation of sediments older than 20 Ma compared to Site U1336 and 807 (Fig. 5a).

The Mg/Ca ratio can also be used for the assessment of diagenetic alteration with elevated values indicating recrystallisation (Delaney, 1989; Delaney and Linn, 1993). Mg/Ca ratios are also species-specific with values of 1–10 mmol/mol for most modern foraminifera (e.g., Rosenthal et al., 1997; Lear et al., 2002; Russell et al., 2004) and 0.1–0.2 mmol/mol for modern coccolithophorids (Stoll et al., 2002).

Recently, Higgins and Schrag (2012) proposed that the Mg content of recrystallised carbonates would be higher than the original bulk carbonate consisting mostly of low Mg/Ca coccoliths. The deepest bulk carbonate sample of Site U1334 (330.6 rmcd, 37 Ma) exhibits elevated Mg/Ca ratios indicating recrystallisation (Fig. 5b, Table S2), but in general Site U1334 is less altered than Site U1336 based on Sr/Ca (Fig. 5a). Site U1336 Mg/Ca decreases with depth in sediments older than 17.4 Ma (below 62.6 rmcd) (Fig. 5b) whereas elevated ratios are reported for recrystallised carbonates (Delaney, 1989; Delaney and Linn, 1993). This may reflect the decrease of pore water Mg/Ca ratios with depth at Site U1336 (see Section 4.1) resulting from exchange with basement basalt.

Mn/Ca ratios can give valuable information about diagenetic changes with high values resulting from Mn–Fe oxyhydroxide or authigenic $MnCO_3$ coatings (Boyle, 1983; Franklin and Morse, 1983; Pena et al., 2005). Recent non-contaminated foraminifera (without coatings) have Mn/Ca ratios of 0.01–0.2 mmol/mol (Rosenthal et al., 1999; Harding et al., 2006).

Site U1337 and U1338 bulk carbonates exhibit higher Mn/Ca ratios than the other PEAT sites and show a peak at about 5 Ma. Correspondence between pore water and bulk carbonate Mn content suggests incorporation from pore water, enriched in Mn^{2+}, as Mn oxide phases are reduced (Fig. 6a). Bulk carbonate Mn/Ca ratios could be biased towards higher values by partial leaching of Mn oxides, although all sites would be affected similarly as the same leaching method was applied throughout. However, the fact that the pore water Mn^{2+} peaks just above the carbonate Mn maxima at U1337 and U1338 suggests higher carbonate Mn/Ca ratios may be explained by Mn-carbonate overgrowths, such as kutnahorite ($Ca(Mn^{2+}, Mg^{2+})(CO_3)_2$) (Boyle, 1983; Pena et al., 2005). Bulk carbonate Mn/Ca values of U1336 increase slightly below 18.2 Ma (72 rmcd) which may also indicate authigenic carbonates and the incorporation of Mn into recrystallised calcites. The pore water Fe^{2+} at the PEAT sites is much higher than the values measured in the bulk carbonates, and Fe/Ca ratios show no corresponding trends between pore water and bulk carbonates (insert of Fig. 6a), supporting the formation of $MnCO_3$ phases rather than the dissolution of the ferromanganese oxides during the leaching process.

4.4. Persistent recrystallisation at Site U1336

In sediments older than 14.7 Ma (below 32.5 rmcd) pore waters of Site U1336 show lower $^{87}Sr/^{86}Sr$ ratios than contemporaneous seawater (Fig. 4c). These lower ratios likely result from upward diffusion of Sr from older carbonates recrystallised deeper in the section. This Sr originating from older carbonates is also evident in bulk carbonates older than 20.2 Ma (Fig. 4c) and suggests active recrystallisation further down in the sediment column.

Recrystallisation modelling performed at other locations (e.g., Richter and DePaolo, 1988; Richter and Liang, 1993) suggests that diagenetic changes in the $^{87}Sr/^{86}Sr$ ratio of bulk carbonates of this age should not be detectable as they would be on the same order of magnitude as the uncertainty of the measurements (about 30 ppm). However, recrystallisation is evident in the $^{87}Sr/^{86}Sr$ ratios of the bulk carbonates and associated pore waters of Site U1336 older than 20 Ma (Fig. 4c). Previous studies at other locations suggested recrystallisation rates decrease exponentially with age and depth (e.g., Baker et al., 1982; Richter and Liang, 1993; Fantle and DePaolo, 2006), but it seems that significant recrystallisation is still ongoing below 100 rmcd at Site

U1336. Today, Site U1336 is located below the CCD resulting in the dissolution of carbonate sediments younger than 12 Ma. In general, recrystallisation modelling at other locations has produced the highest reaction rates for the uppermost 200 m (Hampt Andreasen and Delaney, 2000; Fantle and DePaolo, 2006), corresponding to about 10 Myrs (Richter and Liang, 1993; Hampt Andreasen and Delaney, 2000). At Site U1336 bulk carbonate $^{87}Sr/^{86}Sr$ ratios deviate from contemporaneous seawater in deeper sediments older than 20 Ma suggesting a later phase of recrystallisation (see Figs. 8, 9a and Section 4.1). The recrystallisation coefficients of the model, determined by fitting the pore water properties, also indicate a higher background recrystallisation rate (λ) at Site U1336, as well as a smaller depth increment at which the rate of recrystallisation changes (γ) compared to Sites U1338 and 807 (Tables S4 and S5). Being located near the fracture zone, forced advection (Fantle et al., 2010) may have played a role in the high reactivity at Site U1336. However, without samples from the entire sediment column it is not possible to be more specific about what drives the enhanced reactivity observed at this site.

4.5. $\delta^{88/86}$Sr of pore waters and bulk carbonates

The use of $\delta^{88/86}$Sr ratios in geochemistry is novel and although only a few studies have been published, the $\delta^{88/86}$Sr of modern planktonic foraminifera and coccolithophorids have been measured (Fig. 7b: Krabbenhöft et al., 2010; Böhm et al., 2012). The bulk carbonate samples measured in this study are in good agreement with the range for coccolithophorids (Fig. 7b) which are the main constituents of the bulk carbonates (Section 4.3). The $\delta^{88/86}$Sr ratio of the bulk carbonate of the control sample (U1338A 18H3, Table 2) is in good agreement with the JCp-1 coral reference material but the $\delta^{88/86}$Sr value of the pore water is 0.076‰ higher than the IAPSO seawater (Fig. 7b, Table 2).

The $\delta^{88/86}$Sr of U1336 pore waters increase with depth and age (Fig. 7b, Table 2). This increase is unlikely to derive from basalt or hydrothermal sources as these have lower $\delta^{88/86}$Sr values ranging from 0.25‰ to 0.27‰ (Krabbenhöft et al., 2010). The increase in $\delta^{88/86}$Sr with depth (depth is represented by decreasing $^{87}Sr/^{86}Sr$ ratios) at Site U1336 (Fig. 7b, Table 2) suggests that the recrystallisation of carbonates is associated with an isotopic fractionation process that enriches the pore waters in ^{88}Sr. This ^{88}Sr enrichment indicates that, although less Sr is incorporated into secondary calcite during recrystallisation, the lighter Sr isotope (^{86}Sr) is incorporated preferably leaving heavy pore waters behind. This lighter Sr needs to be locked away in a stable phase that is not dissolved again by further recrystallisation allowing the pore water $\delta^{88/86}$Sr to evolve with recrystallisation. The pore waters of Site U1336 become increasingly isotopically fractionated with depth but show $^{87}Sr/^{86}Sr$ values similar to the associated carbonates suggesting the same Sr source. The $\delta^{88/86}$Sr values of the carbonates do not change noticeably with depth and age since the carbonates have much higher concentrations and mass fraction of Sr than pore waters (by a factor of >100, see Table 2). This results in pore waters being a much more sensitive indicator of isotope fractionation processes than carbonates. Thus our first results of $\delta^{88/86}$Sr from deep sea carbonate sediments indicate that stable Sr isotopes have the potential to identify recrystallised carbonate sediments by their pore water signals.

Precipitation of celestite ($SrSO_4$), as a possible phase of highly fractionated Sr, can be excluded since Site U1336 does not show any extensive consumption of SO_4^{2-} (Pälike et al., 2010) and solution simulations using PHREEQC Interactive Version 3.0.4 (Parkhurst and Appelo, 2013) show that the investigated pore waters are undersaturated with respect to celestite.

Different studies have shown that isotope fractionation depends mainly on the precipitation rate of the carbonates and the crystal surface kinetics (e.g., Fantle and DePaolo, 2007; DePaolo, 2011; Böhm et al., 2012; Higgins and Schrag, 2012). The precipitation rate of secondary calcite during recrystallisation is very low and occurs near equilibrium, so no isotope fractionation is observed (Fantle and DePaolo, 2007; DePaolo, 2011; Böhm et al., 2012). Fantle and DePaolo (2007) pointed out that diffusional effects on Ca isotopes are within the analytical uncertainties. The same should be true for Sr isotopes as Böhm et al. (2012) demonstrated little fractionation at slow precipitation rates (approaching equilibrium) in laboratory experiments and natural systems. Recently, Chao et al. (2013) reported high pore water $\delta^{88/86}$Sr values of 0.82‰ from mud volcanoes in the northern Chu-kou Fault, Taiwan similar to those observed here at Site U1336. Although the chemical composition of the pore waters in this study is very different to those of the mud volcanoes, the isotope fractionation towards higher $\delta^{88/86}$Sr ratios is the same and these authors demonstrated that calcite precipitation along the fluid path was the most likely cause for the heavy pore water $\delta^{88/86}$Sr ratios.

A simple mass balance calculation can be used to estimate the amount of isotopically fractionated Sr that is needed to produce the measured pore water $\delta^{88/86}$Sr values of Site U1336 (Eqs. (1)–(3), Tables 3 and S6). Such heavy pore waters could only be generated if Sr released from the carbonates, enriched in ^{88}Sr, had mixed with the initial pore water that had an assumed $\delta^{88/86}$Sr value of seawater (0.381‰). Unfortunately, no seawater $\delta^{88/86}$Sr data exist for the last 25 Myrs but the $\delta^{88/86}$Sr value of seawater could have changed by a maximum of 0.3‰ during such a period (Vollstaedt et al., 2014). However, such a change in seawater $\delta^{88/86}$Sr does not significantly influence the amount of isotopically fractionated Sr required to produce the observed pore water $\delta^{88/86}$Sr. For simplicity, we assume that the initial bulk carbonate consisted of only coccolithophorids as coccolithophorids represent the main constituent of bulk carbonates. The Sr content of the initial carbonate was estimated by the Sr/Ca range of modern coccolithophorids (1.9–3.2 mmol/mol, Stoll et al., 2002) taking into account the carbonate content of the deepest sample of U1336 (U1336B 20H3: $Ca^{2+} = 358000$ ppm, 89.5 wt % $CaCO_3$, Tables 3 and S6). The Sr/Ca ratios of modern coccolithophorids can be used since the seawater Sr/Ca ratio has not varied significantly over the last 30 Myrs (Sosdian et al., 2012). The calculated Sr content was adjusted to

Table 3
Calculated Sr data for coccolithophorid carbonates.

Sr/Ca ratio (mmol/mol)	Calculated Sr content (ppm)[a]	Sr content adjusted to mass ratio M (ppm)[b]	Calculated percentage of recrystallised Sr (%)[c]	Estimated $\delta^{88/86}Sr_{bulk\ carbonate}$ (‰)[d]
1.9	1487	2781	5.9	0.227
2.0	1565	2927	4.5	0.235
2.1	1644	3074	3.7	0.240
2.2	1722	3220	3.1	0.243
3.2	2505	4684	1.2	0.254

[a] The Sr content (ppm) was calculated from the Sr/Ca ratio given in the first column and the Ca content of sample U1336B 20H3 ($Ca^{2+} = 358000$ ppm).
[b] The calculated Sr content was multiplied by the mass ratio M of sample U1336B 20H3 which was calculated by $M = \rho_{solid} * (1 - \phi)/(\rho_{fluid} * \phi)$ where ρ_{solid} is the density of the calcite with $\rho_{calcite} = 2.7$ g/cm^3 and ρ_{fluid} is the density of the seawater with $\rho_{seawater} = 1.025$ g/cm^3. The porosity ϕ of this sample is 58.5% (Pälike et al., 2010) resulting in $M = 1.87$.
[c] The percentage of the recrystallised Sr input from recrystallisation was calculated using Eq. (1).
[d] The $\delta^{88/86}Sr$ of the recrystallised bulk carbonate was estimated by using Eq. (3).

the mass ratio M of that sample ($M = 1.87$) to take the densities of pore water and calcite, as well as the porosity into account (Table 3). Then the fraction of isotopically fractionated Sr that is released from the bulk carbonates to the pore waters can be calculated by:

$$p_{recrystallised\ input} = \frac{Sr^{2+}_{PW} - Sr^{2+}_{SW}}{Sr^{2+}_{coccolithophorids} - Sr^{2+}_{bulk\ carbonate}} \quad (1)$$

where all Sr concentrations are given in ppm. The Sr^{2+}_{PW} is the Sr content of the pore water, Sr^{2+}_{SW} is the Sr concentration of seawater (7.45 ppm) and $Sr^{2+}_{bulk\ carbonate}$ is the Sr content of the measured bulk carbonate of sample U1336B 20H3 (Table S6). The calculated percentage ranges from 5.9% to 1.2% for low and high Sr content coccolithophorid carbonates (Table 3). The $\delta^{88/86}Sr$ value of this recrystallised Sr contribution from the bulk carbonates (coccolithophorids) was calculated for the deepest U1336 pore water measured giving a $\delta^{88/86}Sr_{recrystallised\ input}$ of 0.78‰ using:

$$\delta^{88/86}Sr_{recrystallised\ input} = \frac{(Sr^{2+}_{PW} * \delta^{88/86}Sr_{PW}) - (Sr^{2+}_{SW} * \delta^{88/86}Sr_{SW})}{Sr^{2+}_{PW} - Sr^{2+}_{SW}} \quad (2)$$

where $\delta^{88/86}Sr_{PW}$ is the stable Sr ratio of the pore water sample U1336B 20H3 (Table S6) and $\delta^{88/86}Sr_{SW}$ is the seawater ratio ($\delta^{88/86}Sr_{IAPSO} = 0.381$‰). The $\delta^{88/86}Sr$ of the recrystallised bulk carbonate can then be estimated by the following equation using the determined $\delta^{88/86}Sr_{recrystallised\ input}$ and the $\delta^{88/86}Sr$ of recent coccolithophorids ($\delta^{88/86}Sr = 0.26$‰; Krabbenhöft et al., 2010):

$$\delta^{88/86}Sr_{bulk\ carbonate} = \frac{\delta^{88/86}Sr_{coccolithophorid} - (x * \delta^{88/86}Sr_{recrystallised\ input})}{1 - x} \quad (3)$$

where x is the fraction of isotopically fractionated Sr that is released during recrystallisation (see Eq. 1). The obtained $\delta^{88/86}Sr$ ratios range from 0.227‰ to 0.254‰ for low and high Sr content coccolithophorid carbonate (Table 3). The average of the measured U1336 $\delta^{88/86}Sr_{bulk\ carbonate}$ of 0.233‰ lies within this range, attesting to the validity of our calculations and is also in agreement with the average $\delta^{88/86}Sr = 0.22$‰ of the major calcifying species (Krabbenhöft et al., 2010). A starting Sr/Ca ratio of 2.0 mmol/mol fits best and results in a recrystallised Sr contribution of the bulk carbonates of 4.5% and $\delta^{88/86}Sr_{bulk\ carbonate}$ of 0.235‰. This Sr/Ca ratio is in accordance with the average of Sr/Ca ratios measured for Sites U1337 and U1338, which are better preserved than U1336 suggesting that the initial Sr/Ca ratio of Site U1336 may have been similar.

Assuming that the initial bulk carbonate had an average Sr content corresponding to a Sr/Ca ratio of about 2.0–2.1 mmol/mol, the release of about 5% of strongly isotopically fractionated Sr during recrystallisation would be sufficient to produce the high $\delta^{88/86}Sr$ values of the pore waters. This suggests the $\delta^{88/86}Sr$ of the carbonates remain unaffected because of their much higher Sr concentrations (with lower $\delta^{88/86}Sr$) compared to the pore waters. The determined recrystallised Sr input ($\delta^{88/86}Sr_{recrystallised\ input} = 0.78$‰) is similar for all analysed pore waters older than 20 Ma, which may indicate a correlation of the isotope fractionation process with the late phase of recrystallisation observed (see Section 4.4).

Diffusive transport in the pore water is most likely responsible for the relatively high $\delta^{88/86}Sr$ signal in the younger part of the sediments as a consequence of a mixing gradient between two end members. Fig. 10 shows a mixing relationship between the $\delta^{88/86}Sr$ and the inverse Sr concentration of the pore waters. The intercept of this mixing line with $\delta^{88/86}Sr$ reveals a source with the same $\delta^{88/86}Sr$ as calculated for the purely recrystallised Sr contribution of the bulk carbonate. The intercept of the mixing line with the inverse Sr concentration gives the seawater Sr concentration as the second end member. The fact that the end members of the mixing relationship are seawater and the recrystallised Sr input validates our calculations.

4.6. Factors influencing recrystallisation

Different factors are believed to influence recrystallisation including sedimentation rates, subsidence, carbonate saturation state of the bottom water and geothermal gradients (Richter and Liang, 1993; Hampt Andreasen and Delaney, 2000). Today, all PEAT sites investigated are below the lysocline, the depth horizon where the rate of

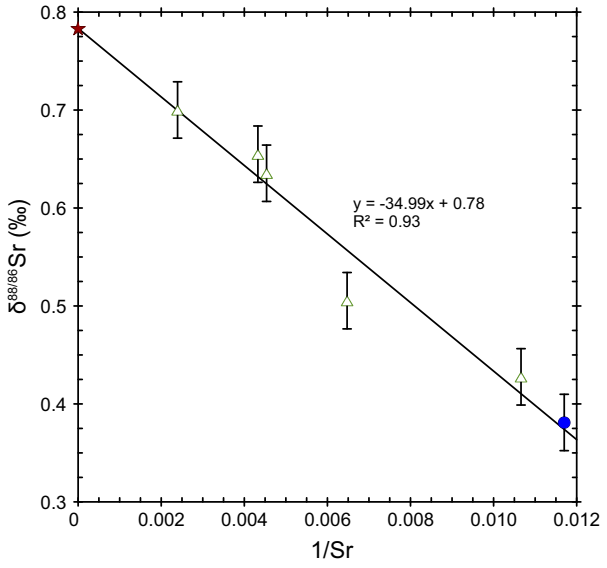

Fig. 10. Inverse of the Sr concentration of Site U1336 pore waters (open green triangles) plotted against $\delta^{88/86}$Sr. The end members for the mixing line are also illustrated: Seawater (IAPSO) (blue cycle) and the $\delta^{88/86}$Sr value of the recrystallised Sr input (red star). Data for the U1336 Sr concentration are from Pälike et al. (2010). (For interpretation of the references to colour in this figure legend, the reader is referred to the web version of this article.)

dissolution of carbonates significantly increases. The lysocline and the CCD have varied over time and were much shallower in the Eocene and deepened drastically at the Eocene–Oligocene boundary and during the early Oligocene, coinciding with the onset of ice sheet growth (e.g., Pälike et al., 2012). When a site subsides below the CCD depends on the rate of subsidence and the age of the crust. Sites U1334 and U1336 subsided below the CCD at around 12 Ma whereas the other sites are still above the CCD (Pälike et al., 2012), but a direct effect of this on the recrystallisation of carbonates at the PEAT sites is unclear. Additionally, although Site U1336 and ODP Site 807 have both experienced intense recrystallisation, Site 807 is still above the CCD, suggesting the saturation state of the overlying bottom water is not a primary control on carbonate recrystallisation. The calcite saturation of the pore waters is even more important for early diagenesis given that undersaturated pore waters tend to dissolve the carbonates and high amounts of organic matter lead to reducing sediments during the remineralisation of organic matter. The total organic carbon (TOC) content of the PEAT sites varies between <0.03% and 0.72% and is highest in the youngest, rapidly accumulated sediments at Sites U1337 and U1338. Such values compare well with benthic lander data from the area (TOC: 0.10–0.99%) (Berelson et al., 1990; Hammond et al., 1996) suggesting the pore waters have calcite saturation values between $\Omega = 0.76$ and 1.36 during early diagenesis and are undersaturated below the CCD (calculated with the carbonate system calculation software CO2SYS from Lewis and Wallace (1998) using the nutrient and carbonate data from Jahnke et al. (1982) and Berelson et al. (1990)).

Sedimentation rates at the PEAT sites do not seem to influence recrystallisation given that sedimentation rates systematically decrease when a site travelled out of the high productivity area (±2°) at the equator. Therefore, Sites U1337 and U1338, as the youngest sites, show the highest sedimentation rates but recrystallisation appears to have been different at these sites.

The lithology of each sedimentary section is also believed to have an impact on recrystallisation with clay-rich sediments reported to be better preserved than carbonate-rich ones (Hampt Andreasen and Delaney, 2000). All PEAT sites investigated are relatively carbonate-rich (Fig. S1, Table S2), but the extent of recrystallisation seems to be related to the carbonate content. The better preserved Site U1337 has on average lower $CaCO_3$ contents with 61.7% (in the ooze sections) compared to Site U1338 with 71.2% (Pälike et al., 2010). Site U1334 shows a slightly higher value than U1338 with 74.4% and is less well preserved compared to Sites U1337 and U1338 (Pälike et al., 2010). Site U1336 has the highest carbonate content reaching 87.3% (Pälike et al., 2010) and is extensively recrystallised, similar to ODP Site 807 with an even higher $CaCO_3$ content of 93% (Kroenke et al., 1991).

The inferred strong geothermal gradient is likely important for the reactivity of the sediment at Site U1336 (see Section 4.1) and the remarkable extent of persistent carbonate recrystallisation. This is most likely due to the proximity (30 km) of Site U1336 to the Clipperton Fracture Zone (Pälike et al., 2010), making the location useful for the study of recrystallisation even if it is a relatively rare case.

5. CONCLUSIONS

The pore water Sr concentrations of the PEAT sites increase with depth due to dissolution of carbonates and the release of Sr from the carbonates to the pore waters during recrystallisation. The $^{87}Sr/^{86}Sr$ ratios of bulk carbonate leachates generally suggest that recrystallisation occurred relatively rapidly (within 1.5 Myrs) as the values are indistinguishable (within 2σ uncertainties) from contemporaneous seawater (McArthur et al., 2001).

The Sr/Ca ratios of the bulk carbonates of Site U1336 are generally lower than those of the other PEAT sites investigated and decrease with depth suggesting more extensive recrystallisation at this site.

In sediments older than 20.2 Ma a late phase of recrystallisation is observed at Site U1336 as the $^{87}Sr/^{86}Sr$ ratios of bulk carbonate leachates and associated pore waters exhibit lower values than contemporaneous seawater. These lower ratios indicate the incorporation of Sr dissolved from older carbonates.

For the first time we document $\delta^{88/86}$Sr fractionation during recrystallisation of deep sea carbonates. Pore water $\delta^{88/86}$Sr values increase with depth at Site U1336 suggesting an isotope fractionation process during recrystallisation where the secondary calcite preferentially incorporates light Sr (^{86}Sr) thus enriching the pore waters in ^{88}Sr. The lighter Sr isotope (^{86}Sr) enriched phase appears to be locked away in a stable phase not released by further recrystallisation. Mass balance calculations show that only a small amount

of Sr in the carbonates (1–6%) must fractionate during recrystallisation to produce the high $\delta^{88/86}$Sr values of the pore waters. Therefore, our first $\delta^{88/86}$Sr results indicate that stable Sr isotopes have the potential to identify recrystallised sediments by their pore water signals. The combination of several Sr parameters (Sr^{2+}, Sr/Ca, $^{87}Sr/^{86}Sr$, $\delta^{88/86}$Sr) indicates that the bulk carbonates of Site U1336 are extensively altered, compared to the other PEAT sites investigated, and also show a late phase of recrystallisation at this more reactive site. Our data suggest a strong geothermal gradient is the primary driver of extensive carbonate recrystallisation at this location.

ACKNOWLEDGEMENTS

This work was funded by the German Science Foundation, DFG, HA 5751/1-1 and HA 5751/2-1 (PEAT). We thank Ana Kolevica, Silke and Folkmar Hauff for laboratory assistance and technical support for the stable Sr isotope measurements. Discussion with Florian Böhm, Jan Fietzke and Volker Liebetrau helped to improve the manuscript. John Higgins kindly provided insights from diffusion reaction modelling. The suggestions of associate editor Silke Severmann and two anonymous reviewers greatly improved the manuscript. We especially thank Matthew Fantle for extensive comments which considerably improved the manuscript.

APPENDIX A. SUPPLEMENTARY DATA

Supplementary data associated with this article can be found, in the online version, at http://dx.doi.org/10.1016/j.gca.2014.10.001.

REFERENCES

Baker P. A., Gieskes J. M. and Elderfield H. (1982) Diagenesis of carbonates in deep-sea sediments-evidence from Sr/Ca ratios and interstitial dissolved Sr^{2+} data. *J. Sediment. Petrol.* **52**, 71–82.

Baker P. A., Stout P. M., Kastner M. and Elderfield H. (1991) Large-scale lateral advection of seawater through oceanic crust in the central equatorial Pacific. *Earth Planet. Sci. Lett.* **105**, 522–533.

Berelson W. M., Hammond D. E., O'Neill D., Xu X.-M., Chin C. and Zukin J. (1990) Benthic fluxes and pore water studies from sediments of the central equatorial north Pacific: nutrient diagenesis. *Geochim. Cosmochim. Acta* **54**, 3001–3012.

Böhm F., Eisenhauer A., Tang J., Dietzel M., Krabbenhöft A., Kisakürek B. and Horn C. (2012) Strontium isotope fractionation of planktic foraminifera and inorganic calcite. *Geochim. Cosmochim. Acta* **93**, 300–314.

Boyle E. A. (1983) Manganese carbonate overgrowths on foraminifera tests. *Geochim. Cosmochim. Acta* **47**, 1815–1819.

Chao H.-C., You C.-F., Liu H.-C. and Chung C.-H. (2013) The origin and migration of mud volcano fluids in Taiwan: evidence from hydrogen, oxygen, and strontium isotopic compositions. *Geochim. Cosmochim. Acta* **114**, 29–51.

Delaney M. L. (1989) Temporal changes in interstitial water chemistry and calcite recrystallization in marine sediments. *Earth Planet. Sci. Lett.* **95**, 23–37.

Delaney M. L. and Linn L. J. (1993) Interstitial water and bulk calcite chemistry, Leg 130, and calcite recrystallization. In *Proc. ODP. Sci. Results 130* (eds. W. H. Berger, L. W. Kroenke, T.R. Janecek, et al.). Ocean Drilling Program. pp. 561–572.

DePaolo D. J. (2011) Surface kinetic model for isotopic and trace element fractionation during precipitation of calcite from aqueous solutions. *Geochim. Cosmochim. Acta* **75**, 2524–2546.

Edgar K. M., Pälike H. and Wilson P. A. (2013) Testing the impact of diagenesis on the $\delta^{18}O$ and $\delta^{13}C$ of benthic foraminiferal calcite from a sediment burial depth transect in the equatorial Pacific. *Paleoceanography* **28**, 468–480.

Elderfield H. and Gieskes J. M. (1982) Sr isotopes in interstitial waters of marine sediments from Deep Sea Drilling Project cores. *Nature* **300**, 493–497.

Elderfield H., Gieskes J. M., Baker P. A., Oldfield R. K., Hawkesworth C. J. and Miller R. (1982) $^{87}Sr/^{86}Sr$ and $^{18}O/^{16}O$ ratios, interstitial water chemistry and diagenesis in deep-sea carbonate sediments of the Ontong Java Plateau. *Geochim. Cosmochim. Acta* **46**, 2259–2268.

Fantle M. S. and DePaolo D. J. (2006) Sr isotopes and pore fluid chemistry in carbonate sediment of the Ontong Java Plateau: calcite recrystallization rates and evidence for a rapid rise in seawater Mg over the last 10 million years. *Geochim. Cosmochim. Acta* **70**, 3883–3904.

Fantle M. S. and DePaolo D. J. (2007) Ca isotopes in carbonate sediment and pore fluid from ODP Site 807A: the Ca^{2+}(aq)-calcite equilibrium fractionation factor and calcite recrystallization rates in Pleistocene sediments. *Geochim. Cosmochim. Acta* **71**, 1039–1056.

Fantle M. S., Maher K. M. and DePaolo D. J. (2010) Isotopic approaches for quantifying the rates of marine burial diagenesis. *Rev. Geophys.* **48**, RG3002. http://dx.doi.org/10.1029/2009RG000306.

Fietzke J. and Eisenhauer A. (2006) Determination of temperature-dependent stable strontium isotope ($^{88}Sr/^{86}Sr$) fractionation via bracketing standard MC-ICP-MS. *Geochem. Geophys. Geosyst.* **7**, Q08009. http://dx.doi.org/10.1029/2006GC001243.

Franklin M. L. and Morse J. W. (1983) The interaction of manganese(II) with the surface of calcite in dilute solutions and seawater. *Mar. Chem.* **12**, 241–254.

Gieskes J. M. (1976) Interstitial water studies, Leg 33, Deep Sea Drilling Project. *Init. Repts. DSDP* **33**, 563–570.

Gieskes J. M. and Lawrence J. R. (1976) Interstitial water studies, Leg 35, Deep Sea Drilling Project. *Init. Repts. DSDP* **35**, 407–424.

Gieskes J. M., Elderfield H. and Palmer M. R. (1986) Strontium and its isotopic composition in interstitial waters of marine carbonate sediments. *Earth Planet. Sci. Lett.* **77**, 229–235.

Gieskes J. M., Gamo T. and Brumsack H. (1991) Chemical methods for interstitial water analysis aboard. JOIDES Resolution. *ODP Tech. Note 15*.

Hammond D. E., McManus J., Berelson W. M., Kilgore T. E. and Pope R. H. (1996) Early diagenesis of organic material in equatorial Pacific sediments: stoichiometry and kinetics. *Deep Sea Res. II* **43**, 1365–1412.

Hampt Andreasen G. and Delaney M. L. (2000) Bulk calcite size fraction distribution and Sr/Ca composition for deep-sea sediments at selected age horizons. *Mar. Geol.* **169**, 185–205.

Harding D. J., Arden J. W. and Rickaby R. E. M. (2006) A method for precise analysis of trace element/calcium ratios in carbonate samples using quadrupole inductively coupled plasma mass spectrometry. *Geochem. Geophys. Geosyst.* **7**, Q06003. http://dx.doi.org/10.1029/2005GC001093.

Higgins J. A. and Schrag D. P. (2012) Records of Neogene seawater chemistry and diagenesis in deep-sea carbonate sediments and pore fluids. *Earth Planet. Sci. Lett.* **357–358**, 386–396.

Jahnke R., Heggie D., Emerson S. and Grundmanis V. (1982) Pore waters of the central Pacific Ocean: nutrient results. *Earth Planet. Sci. Lett.* **61**, 233–256.

Krabbenhöft A., Fietzke J., Eisenhauer A., Liebetrau V., Böhm F. and Vollstaedt H. (2009) Determination of radiogenic and stable strontium isotope ratios ($^{87}Sr/^{86}Sr$; $\delta^{88/86}Sr$) by thermal ionization mass spectrometry applying an $^{87}Sr/^{84}Sr$ double spike. *J. Anal. At. Spectrom.* **24**, 1267–1271.

Krabbenhöft A., Eisenhauer A., Böhm F., Vollstaedt H., Fietzke J., Liebetrau V., Augustin N., Peucker-Ehrenbrink B., Müller M. N., Horn C., Hansen B. T., Nolte N. and Wallmann K. (2010) Constraining the marine strontium budget with natural strontium isotope fractionations ($^{87}Sr/^{86}Sr^*$, $\delta^{88/86}Sr$) of carbonates, hydrothermal solutions and river waters. *Geochim. Cosmochim. Acta* **74**, 4097–4109.

Kroenke L. W., Berger W. H., Janecek T. R., et al. (1991) Site 807. In *Proc. ODP. Init. Repts. 130* (eds. W. H. Berger, L. W. Kroenke, T. R. Janecek, et al.). Ocean Drilling Program. pp. 369–493.

Kryc K. A., Murray R. W. and Murray D. W. (2003) Elemental fractionation of Si, Al, Ti, Fe, Ca, Mn, P, and Ba in five marine sedimentary reference materials: results from sequential extractions. *Anal. Chim. Acta* **487**, 117–128.

Lawrence J. R., Gieskes J. M. and Broecker W. S. (1975) Oxygen isotope and cation composition of DSDP pore waters and the alteration of Layer II basalts. *Earth Planet. Sci. Lett.* **27**, 1–10.

Lear C. H., Rosenthal Y. and Slowey N. (2002) Benthic foraminiferal Mg/Ca-paleothermometry: a revised core-top calibration. *Geochim. Cosmochim. Acta* **66**, 3375–3387.

Lewis E. and Wallace D. W. R. (1998). *Program developed for CO_2 system calculations. ORNL/CDIAC-105*. Carbon Dioxide Information Analysis Center, Oak Ridge National Laboratory, U.S. Department of Energy.

Lyle M., Dadey K. A. and Farrell J. W. (1995) The late Miocene (11-8 Ma) eastern Pacific carbonate crash: evidence for reorganization of deep-water circulation by the closure of the Panama Gateway. In *Proc. ODP. Sci. Results 138* (eds. N. G. Pisias, L. A. Mayer, T. R. Janecek, A. Palmer-Julson and T. H. van Andel). Ocean Drilling Program. pp. 821–838.

Lyle M., Wilson P. A., Janecek T. R., et al. (2002) Site 1218. In *Proc. ODP. Init. Repts. 199* (eds. P. A. Wilson, M. Lyle and J. V. Firth). Ocean Drilling Program.

McArthur J. M. and Howarth R. J. (2004) Strontium isotope stratigraphy. In *A Geologic Time Scale* (eds. F. M. Gradstein, J. G. Ogg and A. G. Smith). Cambridge University Press, Cambridge, pp. 96–105.

McArthur J. M., Howarth R. J. and Baily T. R. (2001) Strontium isotope stratigraphy: LOWESS version 3: best fit to the marine Sr-isotope curve for 0–509 Ma and accompanying look-up table for deriving numerical age. *J. Geol.* **109**, 155–170.

Murray R. W., Miller D. J. and Kryc K. A. (2000) Analysis of major and trace elements in rocks, sediments, and interstitial waters by inductively coupled plasma-atomic emission spectrometry (ICP-AES). *ODP Tech. Note 29*.

Nier A. O. (1938) The isotopic constitution of strontium, barium, bismuth, thallium and mercury. *Phys. Rev.* **5**, 275–278.

Pälike H., Lyle M., Nishi H., Raffi I., Gamage K., Klaus A. and the Expedition 320/321 Scientists. (2010) *Proc. IODP*, 320/321. Tokyo (Integrated Ocean Drilling Program Management International, Inc.). Available at <http://publications.iodp.org/proceedings/320_321/32021toc.htm>.

Pälike H., Lyle M. W. and Nishi H., et al. (2012) A Cenozoic record of the equatorial Pacific carbonate compensation depth. *Nature* **488**, 609–614.

Parkhurst D. L. and Appelo C. A. J. (2013) Description of input and examples for PHREEQC version 3 – a computer program for speciation, batch-reaction, one-dimensional transport, and inverse geochemical calculations: U.S. Geological Survey Techniques and Methods, book 6, chap. A43, p. 497.

Pearson P. N., Ditchfield P. W., Singano J., Harcourt-Brown K. G., Nicholas C. J., Olsson R. K., Shackleton N. J. and Hall M. A. (2001) Warm tropical sea surface temperatures in the Late Cretaceous and Eocene epochs. *Nature* **413**, 481–487.

Pena L. D., Calvo E., Cacho I., Eggins S. and Pelejero C. (2005) Identification and removal of Mn–Mg-rich contaminant phases on foraminiferal tests: Implications for Mg/Ca past temperature reconstructions. *Geochem. Geophys. Geosyst.* **6**, Q09P02. http://dx.doi.org/10.1029/2005GC000930.

Raddatz J., Liebetrau V., Rüggeberg A., Hathorne E., Krabbenhöft A., Eisenhauer A., Böhm F., Vollstaedt H., Fietzke J., Lopez Correa M., Freiwald A. and Dullo W.-Ch. (2013) Stable Sr-isotope, Sr/Ca, Mg/Ca, Li/Ca and Mg/Li ratios in the scleractinian cold-water coral *Lophelia pertusa*. *Chem. Geol.* **352**, 143–152.

Reinhardt E. G., Cavazza W., Patterson R. T. and Blenkinsop J. (2000) Differential diagenesis of sedimentary components and the implication for strontium isotope analysis of carbonate rocks. *Chem. Geol.* **164**, 331–343.

Richter F. M. (1993) Fluid flow in deep-sea carbonate: estimates based on porewater Sr. *Earth Planet. Sci. Lett.* **119**, 133–141.

Richter F. M. (1996) Models for the coupled Sr-sulfate budget in deep-sea carbonates. *Earth Planet. Sci. Lett.* **141**, 199–211.

Richter F. M. and DePaolo D. J. (1987) Numerical models for diagenesis and the Neogene Sr isotopic evolution of seawater from DSDP Site 590B. *Earth Planet. Sci. Lett.* **83**, 27–38.

Richter F. M. and DePaolo D. J. (1988) Diagenesis and Sr isotopic evolution of seawater using data from DSDP 590B and 575. *Earth Planet. Sci. Lett.* **90**, 382–394.

Richter F. M. and Liang Y. (1993) The rate and consequences of Sr diagenesis in deep-sea carbonates. *Earth Planet. Sci. Lett.* **117**, 553–565.

Rosenthal Y., Boyle E. A. and Slowey N. (1997) Temperature control on the incorporation of magnesium, strontium, fluorine, and cadmium into benthic foraminiferal shells from Little Bahama Bank: prospects for thermocline paleoceanography. *Geochim. Cosmochim. Acta* **61**, 3633–3643.

Rosenthal Y., Field M. P. and Sherrell R. M. (1999) Precise determination of element/calcium ratios in calcareous samples using sector field inductively coupled plasma mass spectrometry. *Anal. Chem.* **71**, 3248–3253.

Rudnicki M. D., Wilson P. A. and Anderson W. T. (2001) Numerical models of diagenesis, sediment properties, and pore fluid chemistry on a paleoceanographic transect: Blake Nose, Ocean Drilling Program Leg 171B. *Paleoceanography* **16**, 563–575.

Russell A. D., Hönisch B., Spero H. J. and Lea D. W. (2004) Effects of seawater carbonate ion concentration and temperature on shell U, Mg, and Sr in cultured planktonic foraminifera. *Geochim. Cosmochim. Acta* **68**, 4347–4361.

Schrag D. P., DePaolo D. J. and Richter F. M. (1995) Reconstructing past sea-surface temperatures – correcting for diagenesis of bulk marine carbonate. *Geochim. Cosmochim. Acta* **59**, 2265–2278.

Sexton P. F., Wilson P. A. and Pearson P. N. (2006) Microstructural and geochemical perspectives on planktic foraminiferal preservation: "Glassy" versus "Frosty". *Geochem. Geophys. Geosyst.* **7**, 1–29.

Sosdian S. M., Lear C. H., Tao K., Grossman E. L., O'Dea A. and Rosenthal Y. (2012) Cenozoic seawater Sr/Ca evolution. *Geochem. Geophys. Geosyst.* **13**, Q10014. http://dx.doi.org/10.1029/2012GC004240.

Stoll H. M. and Schrag D. P. (2000) Coccolith Sr/Ca as a new indicator of coccolithophorid calcification and growth rate. *Geochem. Geophys. Geosyst.* **1**, 1–24.

Stoll H. M., Schrag D. P. and Clemens S. C. (1999) Are seawater Sr/Ca variations preserved in quaternary foraminifera? *Geochim. Cosmochim. Acta* **63**, 3535–3547.

Stoll H. M., Rosenthal Y. and Falkowski P. (2002) Climate proxies from Sr/Ca of coccolith calcite: calibrations from continuous culture of *Emiliania huxleyi*. *Geochim. Cosmochim. Acta* **66**, 927–936.

Stout P. M. (1985) Interstitial water chemistry and diagenesis of biogenic sediments from the eastern equatorial Pacific. Deep Sea Drilling Project. *Init. Repts. DSDP* **85**, 805–820.

Tracey J. I., Sutton G. H. and Nesteroff W. D., et al. (1971) Proc. DSDP. Init. Repts. 8. In *DSDP Init. Repts. 8* (eds. J. I. Tracey, G. H. Sutton and W. D. Nesteroff, et al.). Deep Sea Drilling Project.

Vollstaedt H., Eisenhauer A., Wallmann K., Böhm F., Fietzke J., Liebetrau V., Krabbenhöft A., Farkas J., Tomasovych A., Raddatz J. and Veizer J. (2014) The Phanerozoic $\delta^{88/86}$Sr record of seawater: new constraints on past changes in oceanic carbonate fluxes. *Geochim. Cosmochim. Acta* **128**, 249–265.

Von Herzen R. P., Fiske R. J. and Sutton G. H. (1971) Geothermal measurements on Leg 8. In *DSDP Init. Repts. 8* (eds. J. I. Tracey, G. H. Sutton and W. D. Nesteroff, et al.). Deep Sea Drilling Project. pp. 837–849.

Westerhold T., Röhl U. and Wilkens R., et al. (2012) Revised composite depth scales and integration of IODP Sites U1331–U1334 and ODP Sites 1218–1220. In *Proc. IODP, 320/321* (eds. H. Pälike, M. Lyle, H. Nishi, I. Raffi, K. Gamage, A. Klaus and the Expedition 320/321 Scientists). Tokyo (Integrated Ocean Drilling Program Management International, Inc.). http://dx.doi.org/10.2204/iodp.proc.320321.201.2012.

Wilkens R. H., Dickens G. R., Tian J., Backman J. and the Expedition 320/321 Scientists. (2013) Revised composite depth scales for Sites U1336, U1337, and U1338. In *Proc. IODP, 320/321* (eds. H. Pälike, M. Lyle, H. Nishi, I. Raffi, K. Gamage, A. Klaus and the Expedition 320/321 Scientists). Tokyo (Integrated Ocean Drilling Program Management International, Inc.). http://dx.doi.org/10.2204/iodp.proc.320321.209.2013.

Zachos J., Pagani M., Sloan L., Thomas E. and Billups K. (2001) Trends, rhythms, and aberrations in global climate 65 Ma to present. *Science* **292**, 686–693.

Zachos J. C., Dickens G. R. and Zeebe R. E. (2008) An early Cenozoic perspective on greenhouse warming and carbon-cycle dynamics. *Nature* **451**, 279–283.

Associate editor: Silke Severmann